Final Research Performance Progress Report

Grant Award No. N62909-19-1-2013

NON-INVASIVE MEASUREMENT OF SEA ICE THICKNESS USING LOW FREQUENCY EM WAVES

Submitted to:

The Office of Naval Research Global

London, UK

Prepared by:

Anyeshan Limited,

206/A, Tejgaon I/A, Dhaka, 1208,

Bangladesh

Principal Investigator

Dr. Mohammad Ariful Haque

Other Researchers

M. Shifatul Islam • Sadman Shafi • Md. Imrul Hasan

Abstract

Measurement of sea ice thickness is of great importance for safety of navigation and for monitoring the environment, climate and geophysical information. In this research, we propose and investigate a novel concept of measuring sea ice thickness in a non-destructive way through electromagnetic field measurements, and in addition, also estimating the dielectric properties of sea ice. The method involves measuring electric and magnetic fields in the near field zone and estimating the thickness and dielectric properties using deep learning. First, we have developed several analytical methods to simulate an air- sea ice- sea water environment, assuming they form a planar three-layered system. The planewave reflection coefficient, which is a strong function of the thickness and dielectric constant of sea ice bulk, is calculated first, and the expressions are embedded into the source equation of a horizontal electric dipole. A model of sea ice has been developed whose dielectric functions are varied across each layer with changing thickness and age of sea ice and has been used to model the sea ice bulk in the three-layered system. For data acquisition, the source is placed at the air - sea ice interface, and the receiver is swept along a predefined direction across the sea ice bulk. The receiver height can be kept fixed or can be varied as a constant function of wavelength, but for all cases, the *z*-component of the E and H fields appear to show clear dependence with the changing parameters of sea ice. The analytical results are verified with multiple independent calculations and with the help of a finite element simulation software. Afterwards we try to exploit this dependence by forming a deep learning dataset, composed of the normalized field components, operating frequency, and the thickness and dielectric properties of sea ice. A model is fit with the dataset, in order to solve the inverse problem of retrieving the thickness and dielectric properties of ice from the given field data. While evaluating the model, it is found that the thickness and dielectric property estimation is very accurate for the in-domain test set, but the performance degrades for an out-of-domain test set, where the source frequency is outside the training range. We have been able to mitigate this performance degradation by varying the spatial measurement range as a function of wavelength. When we try to estimate the thickness only using the dielectric properties as a priori information, the estimation performance increases even more. Small scale practical experiments have also been performed with wood and ice, whose dielectric properties are very similar to the sea ice dielectric properties at the operating frequencies. The experimental results agree with the intuition developed from the

analytical development and simulation experiments. With a strong theoretical basis, and simulation results as foundation, together with basic experimental validation, this idea can have fascinating prospects for large scale sea ice monitoring.

Table of Contents

1. Introduction:

In this project, we seek to develop a novel nondestructive method of estimating sea ice thickness, with the use of low frequency Electromagnetic waves. At present, there exist multiple methods to determine the thickness of sea ice in the arctic region. However, almost all of the state-of-the-art methods are either destructive or have some practical limitation in large scale monitoring of sea ice. In our work, we explore a new concept of near-field electromagnetic measurements in the sub wavelength region, which appears to show very strong dependencies with both the thickness and the dielectric properties of sea ice. The process to retrieve the actual thickness and dielectric properties of sea ice is mathematically intractable since the inverse relation of the thickness and the dielectric properties with EM field values is notoriously complicated. For such complex cases, recently deep learning models provide the pathway to estimate the inverse relation between the estimation parameter(s) and the extracted variable(s). Thereby we propose the use of deep learning to estimate not only the thickness, but also the dielectric properties simultaneously, which has never been done before.

The use of low frequency EM waves to estimate the sea ice parameters have some advantages over the state-of-the-art methods. First of all, in GPR based thickness estimations, the presence of brine packets inside the sea ice bulk induces strong undesirable scattering, which ends up in erroneous estimations. Low frequency EM waves circumvent this limitation, as at such low frequencies, the sea ice bulk would appear as a homogeneous medium, thereby overcoming the limitation of scattering. Furthermore, low frequency responses are often monotonic and therefore the relation with thickness and dielectric variation is not strongly nonlinear, which is often a good trait to have when using estimation techniques.

2. Objectives of the Project:

Based on the aforementioned facts, the project objectives are as follows:

- Develop an analytical model of sea-ice layer response due to low frequency EM waves
- Investigate the feasibility of sea-ice thickness measurement using low frequency EM waves
- Develop a deep learning neural network methodology for noninvasive measurement of sea-ice thickness

3. Proposed Methodology:

The schematic diagram of the proposed approach is shown in Fig. 1. The transmit dipole antenna will emit low frequency EM waves and the response from different interface boundaries will be recorded by the receiver at different receiver points. We would use a horizontal electric dipole antenna as a transmitter, which would excite both TM and TE waves. The waves respond with the thickness and dielectric variation of sea ice. These receiver points are directed along a particular direction, gradually increasing distance from the source, with keeping the receiver height fixed. This sweep of the receiver along a predefined direction is termed as "radial sweep" from the source. After extracting the field data from the radial sweep measurements, we feed them into a deep learning model to train and learn the thickness and dielectric variation, and later use the model to test the performance over unknown field data.

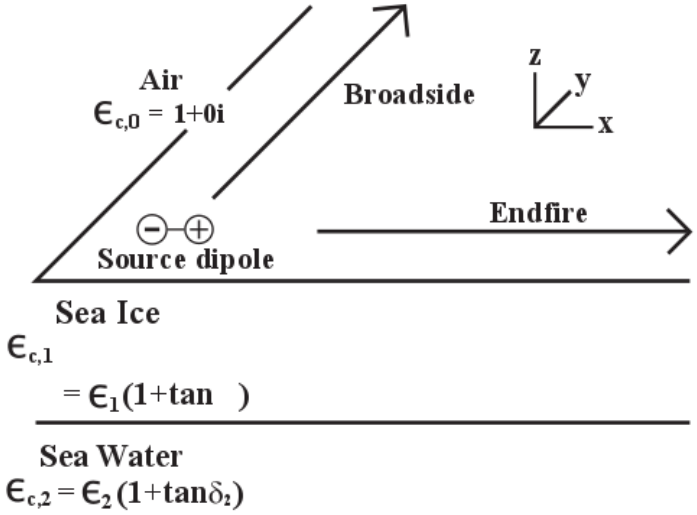

Fig. 1: Schematic arrangement of the radial sweep method over sea ice

4. Statement of Work:

The work was divided into the following tasks:

Task 1:

Objective: Development of an analytical model of the response characteristics of sea-ice media due to low frequency EM waves

Description: We would develop an analytical model to solve the electromagnetic fields due to different types of dipole antennas in the presence of layered sea-ice and seawater media. The objective of this task was to explore the quantitative relationship between sea-ice thickness and

E-field response. The effects of both anisotropy and layering had to be considered and the model would be expanded to n-layer system with arbitrary position of the source dipole in any medium. Again, receiver often could be exposed to different sources of noise and the noisy condition will be taken into account in the study.

Completion criteria: After the completion of the task, we would get an analytical model that defines the quantitative relationship between E-field response and sea-ice thickness.

Task 2:

Objective: Validate the developed analytical model using finite-element simulation and experimental data

Description: We had to develop a virtual model of the sea-ice and seawater media using COMSOL, a high-fidelity finite-element computer simulation software. We would generate the simulated data using this virtual model by placing dipole antennas in appropriate locations and solving the model for appropriate boundary conditions. The data from the COMSOL model would be analyzed to verify the quantitative relationship between E-field response and sea-ice thickness obtained from the analytical model. If experimental data is made available to us by ONRG through the experiments conducted by Dr. Bjorn Erlingsson or from any other suitable source, we would validate our model using that real dataset.

Completion criteria: After the end of the task, we would be able to verify our analytical model using simulation and real data.

Task 3:

Objective: Develop a deep learning neural network methodology to measure sea-ice thickness

Description: Deep learning neural network is a powerful set of techniques that enables a computer to learn from observational data. Currently, it is the state-of-the-art methodology in many scientific domains surpassing the performance of traditional techniques by significant margin. We would develop a deep learning methodology in order to measure the ice thickness using the features of the received EM signal. The developed analytical and simulation models in task 1 and 2 would be utilized to generate synthetic data and augment experimental data to prepare the train, validation and test dataset for the deep learning model. We would also delineate performance analysis of our method with relevant data.

Completion criteria: After the end of the task, we would get a data driven model to predict sea-ice thickness from E-field response

Task 4: Methodology Demonstration

Finally, we would develop an engineered system to demonstrate the validity of our methodology for measurement of sea-ice thickness. The advantage of using deep learning technique is that the performance of the model can be improved continuously by acquiring more E-field data and adding multiple data types such as surface texture from infrared imagery and freeboard measurement with the E-field response.

5. Achievements:

5.1 Developing the analytical expressions of electromagnetic fields over layered media:

In order to discuss the feasibility of our proposed method of sea ice thickness estimation from near-field measurement, we needed to develop the analytical foundation of the proposition. Result obtained through analytical computation serves as the primary baseline of what to expect when we extract near-field measurement data over an air sea ice sea water environment (see Fig.1). To do that, first we developed the analytical framework for generalized three layered systems and approached to characterize the middle layer, which can have arbitrary dielectric values. The analytical treatment has been divided in the following steps:

5.1.1 Determination of the planewave reflection coefficient over layered media:

The first step to solving the analytical problem was to determine the planewave response of the three-layered air-sea ice- sea water systems. The information regarding the thickness and the dielectric properties of the sea ice lies in the "Generalized planewave reflection coefficient", which can be both TM and TE reflection. For an n layered system, this generalized reflection coefficient is recursively computed bottom up [1] using $n-1$ recursions.

The TM reflection is a strong function of the sea ice thickness and dielectric properties, whereas the TE reflection is a strong function of the sea ice thickness only. We take advantage of this fact and extract one TM and one TE excited fields, so that we can make good estimations of all the characterization parameters of sea ice [2].

5.1.2 Developing a low frequency EM model of sea ice:

Initially, we developed a crude, low frequency electromagnetic model of sea ice [3] where the sea ice has been considered as a gradually varying dielectric with thickness changing with porosity and salinity across each layer. We have developed three different models of sea ice,

with increasing complexity and nonlinear relation between the dielectric properties and the associated physical parameters. One of the models also takes into account the effect of age of the sea ice on its properties. One-year-old ice (also known as “frazil" ice) has higher salinity than multiyear ice, and that creates a noticeable difference between the conductivities of frazil ice and multiyear ice.

Later on, we developed a more refined model of sea ice using the experimental data published in [4]. We used the updated model to investigate further complex responses of sea ice in the presence of varying EM fields at different frequencies.

5.1.3 Calculation of the Sommerfeld integrals:

The most common electromagnetic sources available are spherical in nature. In order to fit the planewave reflection coefficients into the spherical wave expressions, we needed to decompose the spherical source into an integral superposition of a circular wave and a planewave along the direction of stratification. We have done this by using the “Sommerfeld Identity”, and such integral representations are termed as Sommerfeld integrals. While evaluating the Sommerfeld integral for dipole radiation, several singularities and branch points had arisen. We have taken into account these singularities and branch points when employing any method to compute the integral. Though computation of Sommerfeld integral is discussed in the literature for different contexts, no known work has addressed the problem at near-field region for low-frequency EM waves.

5.1.4 Evaluation of electric and magnetic fields in the presence of three-layered systems

After properly evaluating the Sommerfeld integrals, we computed the electric and the magnetic field components at any point due to radiation from a dipole antenna with arbitrary orientation. The simulation codes were developed for the Horizontal electric dipole configuration, which excites both TM and TE reflections. Among 12 different field components, we put emphasis on the TE component of the magnetic field and the TM component of the electric field, since these two were the only two decoupled waves and the other 10 components are dependent on them. We apply the sea ice model which has been developed and observed the field response with changing thickness and dielectric properties of sea ice.

5.2 Proposition of a new method "Near field interferometry" to determine the field relation with thickness and dielectric properties of sea ice:

5.2.1 The near field interferometry method to characterize lossy dielectrics like sea ice

After observing the near-field dependencies of sea ice with changing thickness and dielectric properties, we proposed a field measurement method to observe the change of EM field values with varying thickness, loss tangent and dielectric constant. We name the method as "Near field interferometry", where the source is kept at the interface between the air and sea ice sample. The receiver is placed at different points along the broadside direction for determining the z-component of the magnetic field. The receiver height was fixed at 2 meters, and the location was varied from 2 meters to 20 meters from the source along the preferred direction. We have noted strong and monotonic dependencies for the magnetic field with changing thickness of sea ice [1]. Later on, in [5] we have found that the E fields along the endfire direction also show considerable variation with not only the thickness but also the dielectric and loss tangent variation of sea ice (see Fig. 2).

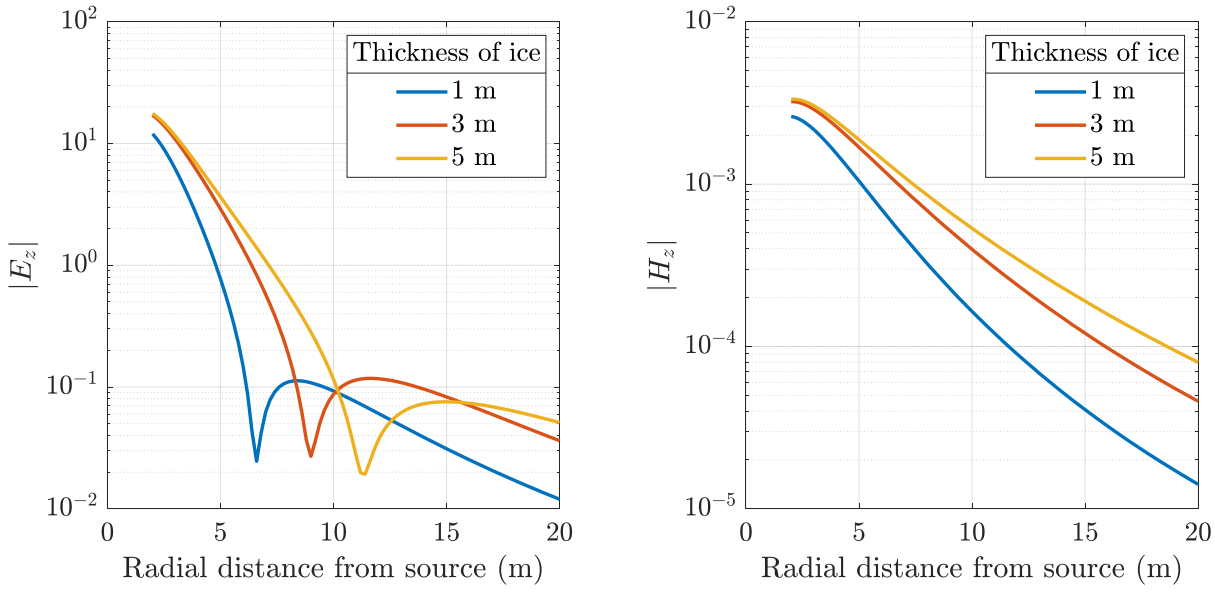

Fig 2. Analytically computed magnitude of the z-component of the E and H fields of the air-sea ice-sea water system, in the near field interferometry approach. The frequency is 5 MHz, $\epsilon_{ice} \approx 7.5$, $\tan \delta_{ice} \approx 0.55$, the bottom layer is highly conductive sea water.

5.2.2 Exploring the theoretical limits of the measurement of dielectric (sea ice) thickness:

In [1] we have also presented the theoretical lower and upper limits of the dielectric loss tangent value, below (above) which the near-field dependencies of the dielectric subsurface tend to subside. It has been shown that the loss tangent values of sea ice lie in the perfect place, neither too much or too little, and the field values vary maximally with both the thickness and dielectric properties of sea ice.

5.3 Verification of the analytical expressions:

5.3.1 Numerical Implementation

Since the analytical expressions for near-field measurement were not explored before and there was no experimental data to verify the computational results, we chose to verify the Sommerfeld-integral based analytical results, by using several methods: (i) The modified Simpson's rule, (ii) the DFT rule, (iii) the Gauss-Kronrod method, (iv) the Romberg-Shanks method, and (v) the "emmod" software package to cross check and validate the analytical results. The entirely different computational methods provided identical results which ensure that the analytical results are accurate.

5.3.2 Finite element simulation

As a next step to verification, we used COMSOL Multiphysics, a finite element software, to simulate a three-layered system like the ones developed analytically. The COMSOL simulation results agreed with very high precision with the analytical results (see Fig. 3a) [5]. The near E-field showed distinct maxima and minima location, followed by a monotonic decrease of the signal amplitude directly related to the thickness and permittivity of the middle layer. The location of the minima is also showed to be directly proportional to the thickness of the middle layer (see Fig. 3b).

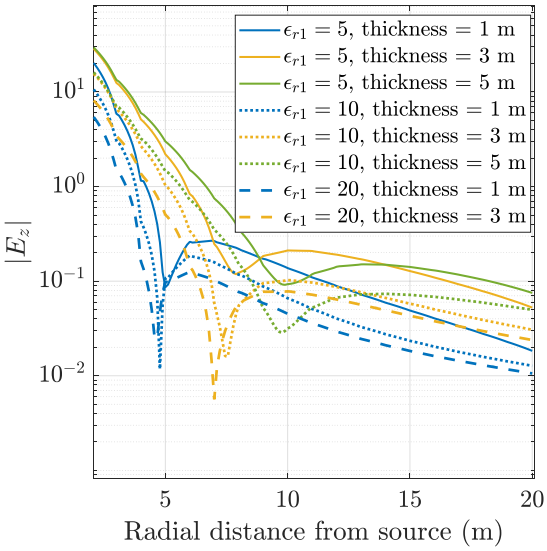

(a)

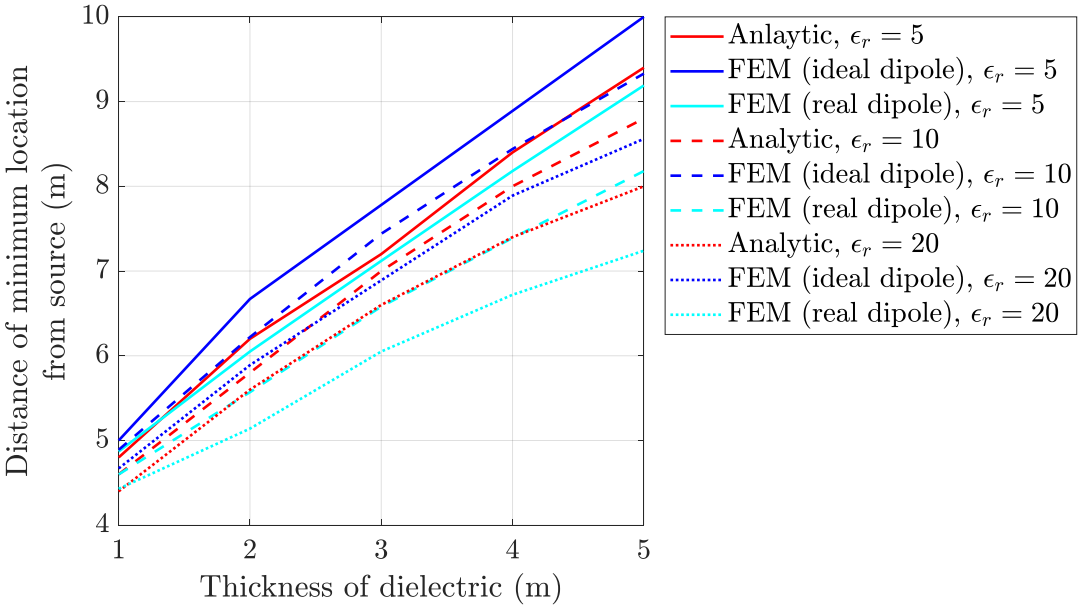

(b)

Fig 3. (a) Comparison between analytical and FEM data for different thickness and dielectric values of the middle layer, (b) A proportional relation of the minima locations with varying thickness of the middle layer. [5]

5.4 Estimation of thickness and dielectric properties of sea ice using a neural network model:

5.4.1 Solution of inverse problem for dielectric characterization:

Having developed multiple computational and simulation methods to determine the field response in the presence of three-layered media and establishing a high degree of correlation between the EM field values and the dielectric properties, we approached to develop a neural network based deep learning method to solve the inverse problem i.e., to estimate the thickness, permittivity and conductivity values of the dielectric from its associated field values [6]. The frequency dependent characteristics of the middle substrate layer were also considered so that it would resemble a practical geophysical dielectric.

The deep learning model consists of a three-layered multi-layer perceptron (MLP) network with fully connected layers. The normalized field values were fed into the network to train the model. The accuracy of the model was evaluated on the held-out test set considering a fully conductive or a regular dielectric bottom layer. The trained model could estimate the permittivity, conductivity and the thickness of both middle and bottom layers with very low error [6].

5.4.2 Estimation of thickness and dielectric properties of sea-ice from near-field measurements:

After training and evaluating the model on a generalized planar three-layered system, we proceeded to estimate the characterization parameters of sea ice. Sea ice permittivity and loss tangent are strong functions of the operating frequency, temperature and salinity, and the dispersion curve of sea ice has been extracted from [6]. Similarly, the bottom layer has been modeled using sea water properties which are also a strong function of frequency, temperature, and salinity. The top layer, where the source dipole is kept, is air, which is modeled with $\epsilon_0 = 1, \tan\delta_0 = 0$.

After modeling a complex three-layered system for sea ice, we proposed two methods of data acquisition technique with the near-field measurement. The first one is termed as the “Fixed radial sweep” and the second one is termed as “Scaled radial sweep”. In the first method, the height of the receiver and its distance from the source are always fixed independent of the wavelength, whereas in the second method the receiver distance is scaled with the wavelength by a constant multiplication factor. Our analysis shows that the scaled radial sweep method is

less dependent on frequency, and more suitable for estimating the sea ice thickness and dielectric properties over a wide band of frequency.

5.5 Performance evaluation of the proposed method for measuring the sea ice thickness and dielectric properties

After laying down the methods to estimate the sea ice thickness and dielectric properties, we seek to investigate the performance of the two proposed methods. We reported [2] that the fixed and scaled radial sweep methods both show extremely low error when the frequency of the test data falls inside the training limits. The estimation performance of the fixed radial sweep degrades rapidly when the test frequencies are outside the training limits, although this degradation of the scaled sweep is much less for the same amount of frequency deviation (see Fig. 4).

Afterwards, we used the dielectric constant and loss tangent values as input training data, assuming we know these values as priori. For this case, the estimation of thickness improves further to a near zero error (see Fig. 5).

It is worth noting that the amount of the FEM simulation data was significantly less than that of the analytical data, and therefore the deep learning models trained only on the FEM simulation data tend to overfit and perform with much less accuracy.

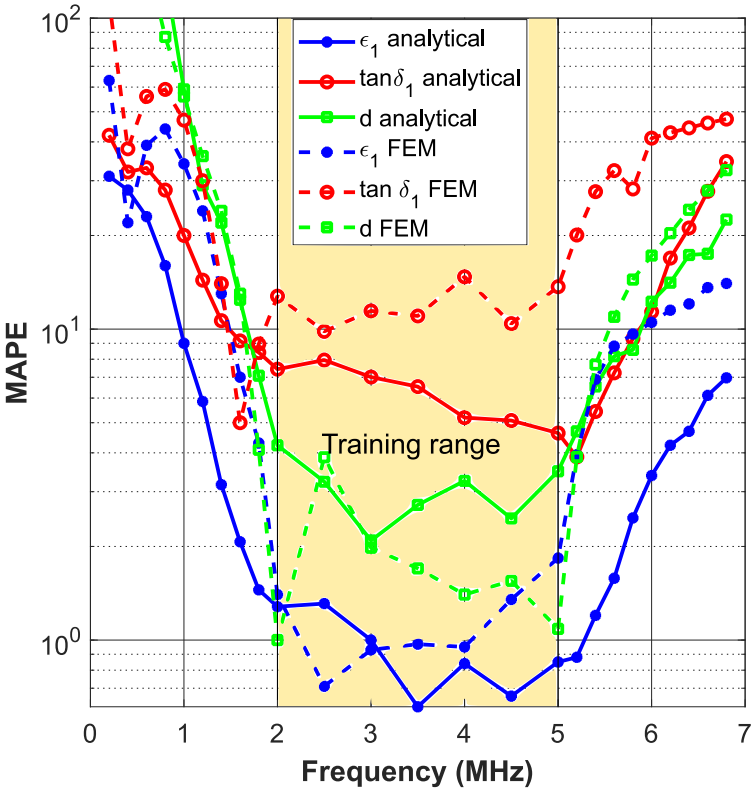

(a)

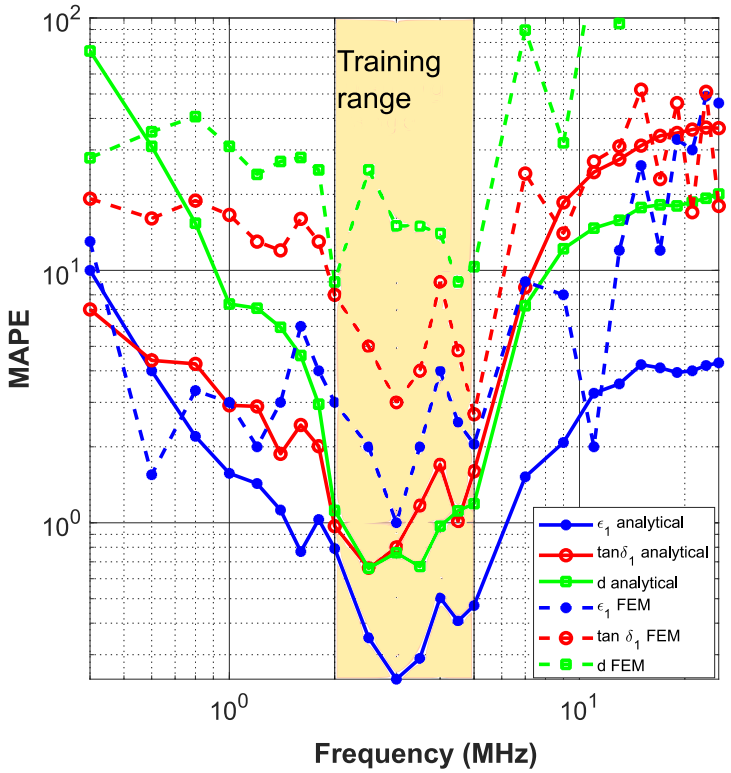

(b)

Fig 4. Estimation error of ϵ_1, tan δ_1 and d for the test dataset at different measurement frequencies: (a) fixed radial sweep (b) scaled radial sweep.

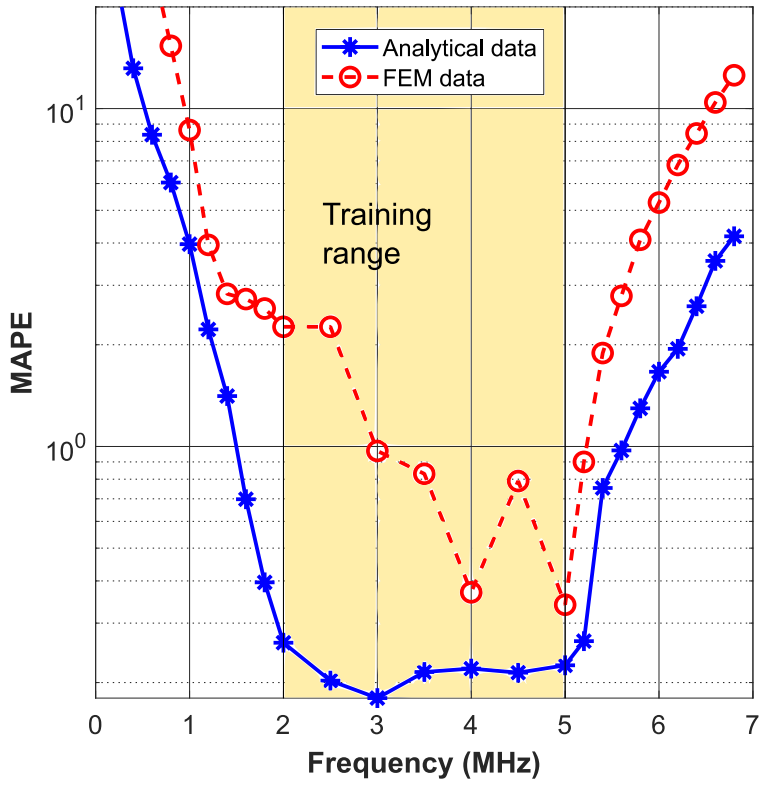

(a)

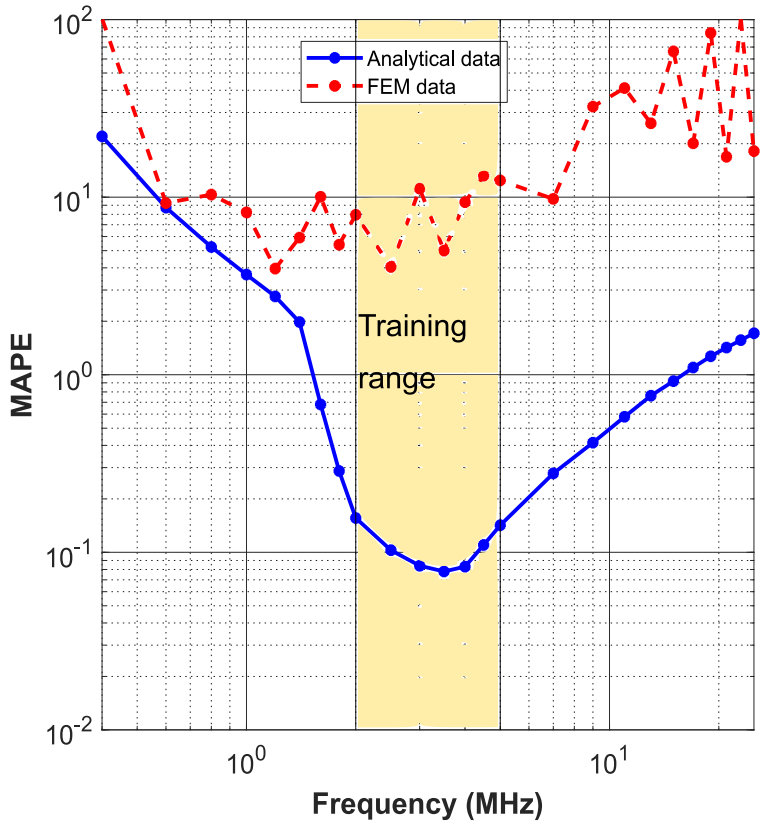

(b)

Fig 5. Estimation error of determining the sea ice thickness using a priori dielectric information: (a) fixed radial sweep (b) scaled radial sweep

5.6 Experimental demonstration of near-field dependency:

Finally, we seek to experimentally verify the near-field dependency of dielectric thickness, conductivity and permittivity values through experiment, and try to verify the claim that the field value depends on the thickness of the middle layer, especially when the bottom layer is a very highly reflecting ground. We used two different dielectric substrate materials for our experiments - wood and ice.

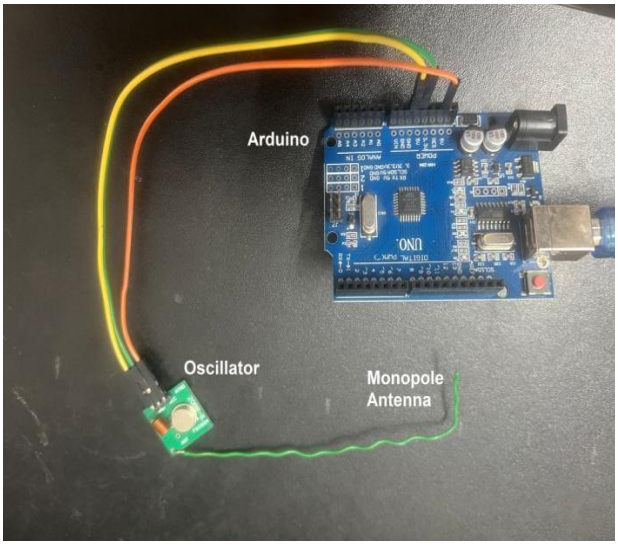

(a) The transmitter monopole, connected with an RF oscillator

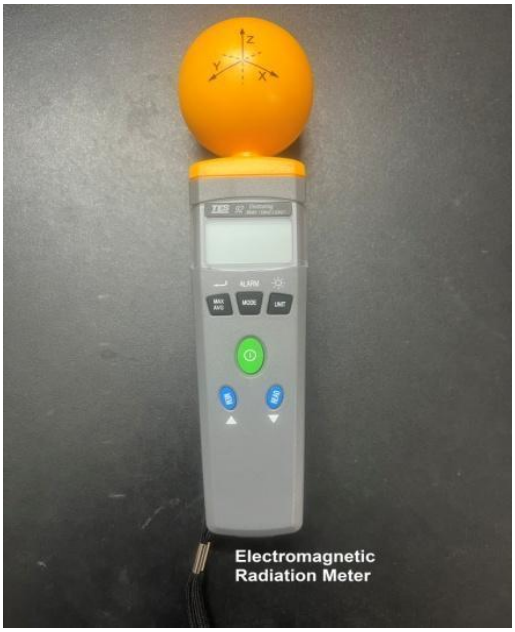

(b) The receiver, TES Electrosmog meter.

(c) Stacked arrangement of the wood sample for experiment

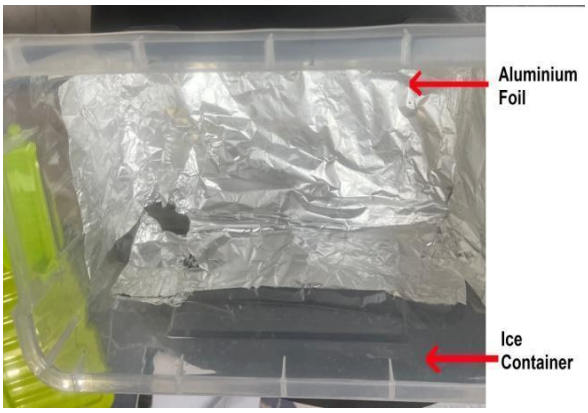

(d) Ice container arrangement for the experiment

Fig 6: Apparatus for the near-field measurement experiment

Transmitter and receiver

The source antenna is a monopole antenna, connected with an RF 433MHz Transmitter module which has a frequency of 433 MHz (see Fig. 6a). At this frequency, the dielectric constant and loss tangent values of sea ice, regular ice and wood are very close to each other [7]. The receiver is an EMF meter, which can operate between 50 MHz to 2.5 GHz (see Fig. 6b). The transmitter was powered using Arduino Uno.

Wood substrate

For the wood sample, multiple slabs of wood with dimensions $80 \times 80 \times 3.5\ \text{cm}^3$ have been cut. Two slabs of wood samples were stacked over one after another. The bottom wood surface is covered with Aluminum foil to emulate a highly reflective ground. The monopole is placed on the top surface and the EMF meter is swept along the broadside direction from 10 cm to 20 cm in front of the source.

Ice substrate

For the ice sample, a plastic container with dimension $50 \times 35 \times 25\ \text{cm}^3$ is used to form ice slabs. The inside of the container was first covered with aluminum foil to facilitate reflection. Two slabs of ice were formed with thickness 3.5 cm and 5.2 cm. Once again, the H field values are computed along the broadside direction with the receiver being swept from 10 to 20 cm in front of the source.

Results

The resulting H-field for the two configurations are shown in Fig. 7. From the figures we can see that the magnitude value is directly related with the thickness of the wood or ice sample, and the larger the thickness, the more the magnitude of the field values. The magnitude of the H-field also decreased with the distance from the source. These observations agree with our simulation results presented in [2]. However, the experimental arrangement was done in a crude environment and we have faced multiple shortcomings while taking measurements. These are:

(a) It was not possible to create an ideal dipole, and therefore we had to use an approximate short monopole antenna.

(b) The measured data was not always stable, and therefore we took the statistical mode.

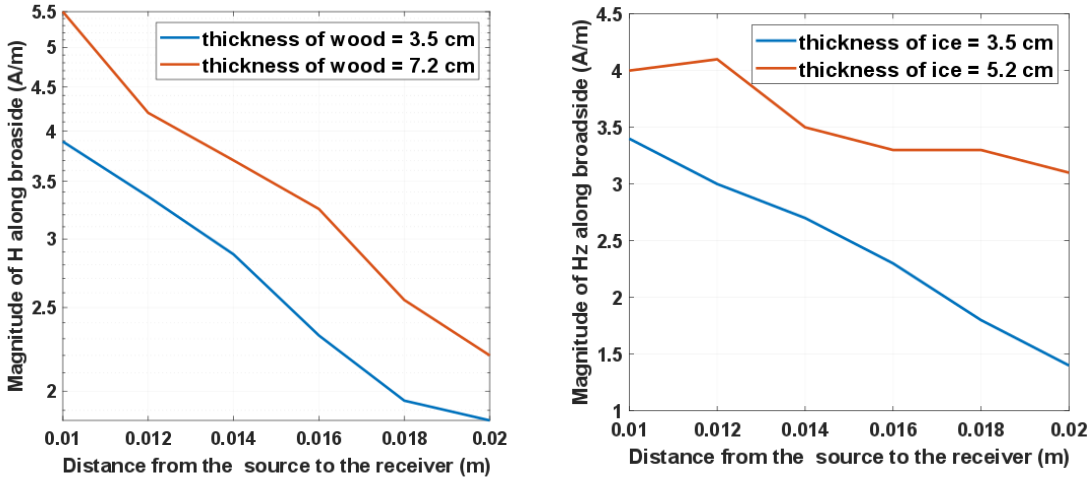

(a) (b)

Fig. 7: Experimental results of the magnetic field in the near field zone for (a) wood and (b) ice samples, for different thickness values

5.7 Publications:

1. M. S. Islam, S. Shafi, and M. A. Haque, "Electromagnetic characterization of sea ice using low frequency electromagnetic waves," in Proc. The 7th Advanced Electromagnetics Symposium (AES 2019), Lisbon, Portugal, Jul. 2019, pp. 290–29
2. M. S. Islam, S. Shafi, M. I. Hasan, and M. A. Haque, "Low-frequency near-field interferometry for characterization of lossy dielectric and an investigation on sea ice." *IEEE Transactions on Geoscience and Remote Sensing* 60 (2020): 1-11.
3. M. S. Islam, S. Shafi, and M. A. Haque, "Development of an experimental model of low frequency dipole radiation in the presence of multilayered structures." *SoutheastCon 2021*. IEEE, 2021.
4. M. S. Islam, S. Shafi, and M. A. Haque, "Low-Frequency Electromagnetic Characterization of Layered Media Using Deep Neural Network." *2021 International Symposium on Antennas and Propagation (ISAP)*. IEEE, 2021.
5. M. S. Islam, S. Shafi, and M. A. Haque, "Estimation of Thickness and Dielectric Characteristics of Sea Ice from Near-Field EM Measurements using Deep Learning". Submitted to: *"IEEE Transactions on Instrumentation and Measurements"*. June 26, 2022.

5.8 Presentations

Mohammad Ariful Haque, “Non-invasive measurement of sea ice”, presented in *Arctic Portfolio Seminar Series: Oceanography May 10-14*, 2021

6. Conclusion

During the project implementation period, every task has been addressed and completed. Noteworthy information is disseminated to the community of interest through multiple conferences and journals. The low frequency near-field responses of sea ice over sea water is examined analytically and verified with suitable finite element analysis. The experimental prototype of wood and ice samples also appear to agree with the general expectations; however, both the experiments are done using ordinary devices in sub-optimal environments. Further experiments with proper transmitter and receiver over natural or synthetic sea ice samples are needed in laboratory scale to gain even more practical sense, and to generate real field data for deep learning purposes. Overall, after the project, it has been found that the near-field measurement over sea ice can simultaneously estimate the thickness and the dielectric properties of the ice bulk, which is a completely novel idea and can have fascinating prospects in the study of sea ice monitoring.

References:

1. M. S. Islam, S. Shafi, M. I. Hasan and M. A. Haque, “Low-frequency near-field interferometry for characterization of lossy dielectric and an investigation on sea ice.” *IEEE Transactions on Geoscience and Remote Sensing* 60 (2020): 1-11.
2. M. S. Islam, S. Shafi, and M. A. Haque, “Estimation of Thickness and Dielectric Characteristics of Sea Ice from Near-Field EM Measurements using Deep Learning”. Submitted to: *“IEEE Transactions on Instrumentation and Measurements”.*
3. M. S. Islam, S. Shafi, and M. A. Haque, “Electromagnetic characterization of sea ice using low frequency electromagnetic waves,” in Proc. The 7th Advanced Electromagnetics Symposium (AES 2019), Lisbon, Portugal, Jul. 2019, pp. 290–29
4. F. L. Wentworth and Mo Cohn. “Electrical properties of sea ice at 0.1 to 30 Mc/s.” *J. Res. NBS* 68 (1964): 681-691.
5. M. S. Islam, S. Shafi, and M. A. Haque, “Development of an experimental model of low frequency dipole radiation in the presence of multilayered structures.” *SoutheastCon 2021*. IEEE, 2021.

6. M. S. Islam, S. Shafi, and M. A. Haque, “Low-Frequency Electromagnetic Characterization of Layered Media Using Deep Neural Network.” *2021 International Symposium on Antennas and Propagation (ISAP)*. IEEE, 2021.
7. William L. James, “Dielectric properties of wood and hardboard: variation with temperature, frequency, moisture content, and grain orientation.” Vol. 245. Department of Agriculture, Forest Service, Forest Products Laboratory, 1975.

Appendix A: Estimation of Thickness and Dielectric Characteristics of Sea Ice from Near-Field EM Measurements using Deep Learning

Estimation of Thickness and Dielectric Characteristics of Sea Ice from Near-Field EM Measurements using Deep Learning

M. Shifatul Islam, Sadman Shafi and Mohammad Ariful Haque

***Abstract*—The near and far field EM responses over layered media has long been exploited in diversified applications such as remote sensing, monitoring and communication. In this work, we utilize the near field dependence of the EM fields of a three layered structure resembling air-sea ice-sea water to estimate the thickness and dispersion characteristics of sea ice using deep learning technique. We explore two key methods of field measurement termed as the fixed and scaled sweep methods, which employ fixed or variable length spatial sampling for different radiation frequency. A synthetic training dataset has been generated (using analytical computation and FEM simulation) in the low MHz band, which is used to train a deep learning model. The model is tested on different test datasets with frequencies inside, below and above the training limits. Both measurement methods work well for test frequencies inside the training range, whereas the scaled sweep method performs significantly better for test frequencies outside the training band. Later, we investigate the problem of determining sea ice thickness assuming a priori knowledge of sea ice dielectric parameters, and results show that the model estimates the thickness of the sea ice bulk with very low error.**

***Index Terms*—sea ice, dispersive media, thickness measurement, neural network application, modeling, electromagnetic fields, electromagnetic measurements, electromagnetic propagation in dispersive media, dipole radiation.**

I. Introduction

The study of electromagnetic field variations with the changing thickness and dielectric properties of geophysical substances (also sometimes termed as substrate) is known as "interferometry". Far field interferometry has widely been used in determining the field response in the presence of different geophysical substrates. [1]–[5] The relative location of the peak and troughs, and the sharpness of the interference curve yield crucial dependencies on the dimensions and dielectric properties of the substrate under interest. It is well known that this method is not suitable for determining the properties of substrate when its thickness is very small compared to the wavelength, and when the loss is several orders higher. For this case, interference patterns diminish very quickly, which has been studied thoroughly in [2]. For such types of dielectric configurations, [6] proposed an idea of "near field interferometry", where an analytical study of near field magnetic fields show clear monotonic dependence with both thickness and dielectric properties of the substrate, whose thickness is in the subwavelength regime. The study was progressed further in [7], where the analytical results were verified using a finite element model, with the additional exploration of the electric field dependencies. It was shown that electric fields show a stronger, and more non linear dependence with thickness, and show distinctive maxima and when the field values are measured very close to the top interface. The study also showed that the positions of those extremes are directly related to the thickness and the dielectric constant of the substrate. A later work [8] tried to solve the inverse problem of actually retrieving the constituent parameters from the field values, using deep learning to learn the established clear correlations of the near field patterns with the substrate properties. The study used arbitrary dielectric constants for different planar three layered structures, and demonstrated that it is indeed possible to extract the thickness and dielectric properties for more than one layer of stratification, using simplified deep learning regression methods. However, the estimation performance degraded with more number of layers, and with addition of different level of noise.

In the theoretical development of both far and near field interferometry, particular attention has been given to the case where the bottom layer is highly reflective [1], [3], [6], [7]. For near field condition, it is shown that fields vary significantly with the substrate characterization parameters if the bottom layer reflects all the waves from the bottom interface; and consequently it gives an obvious advantage for solving the inverse problem [8]. This observation motivated us to use this method to characterize sea ice bulks. In the MHz range, the ground (sea water) works as a very lossy medium with reflection coefficient near unity [9] and the air-sea ice-sea water environment would form a three layered system, over which the near field interferometry is supposed to work. However, sea ice is a more lossy dielectric [10]–[12] as compared to regular ice, snow or glacier [4], [5], [10], [13], which is primarily attributed to the presence of saline brine packets trapped inside the sea ice bulk. This increases both the dielectric constant and loss tangent values of sea ice resulting in a more complex dispersion relation. Hence, the characterization of sea ice can be more challenging than

M. Shifatul Islam is with Anyeshan Limited, Dhaka, Bangladesh. E-mail: shifatul@anyeshan.com

Sadman Shafi is with Anyeshan Limited, Dhaka, Bangladesh.

Mohammad Ariful Haque is with the Department of Electrical and Electronic Engineering, Bangladesh University of Engineering and Technology, Dhaka, Bangladesh.

a general three-layered dielectric structure discussed in [8]. In the literature, there do exist methods which can measure sea ice dielectric properties [10]–[14] and thickness [15]–[22] independently with or without electromagnetic waves. Among these methods, the EM sounding [22] is a well-known technique which uses a transmitter and a receiver coil; where the transmitter-sea water interaction induces a secondary field in the receiver coil and it exploits the theoretical relationship between the received field strength and the sea-ice thickness. The relationship is expressed as a complex integral representation with a Bessel function of the first kind of order zero, which can be solved numerically to estimate the thickness for given conductivities of the ice and water. In our work, we present a novel method of simultaneous estimation of both sea ice thickness and dispersion relation using deep neural networks (DNN) which would open up a completely new paradigm in large scale monitoring of polar marine environment. The DNN is trained on near field data with a defined range of frequencies; the choice of frequency is such that the thickness of sea ice falls in the subwavelength dimensions. In addition to characterizing sea ice from low frequency measurements, we also explore the frequency mismatch between the training and test data. In other words, we want to determine the possibility of characterizing sea ice parameters even when the range of frequencies at inference time is different from those in the training dataset. If this is a plausible case, we can actually train a deep learning model with a limited training dataset and use this model to characterize sea ice over a wide range of experimental frequencies. We will present the results in a later section, and show that the idea is feasible if we define the measurement method in a wavelength scaled way.

We divide the rest of the paper into three sections. In section II, we discuss the feasibility of the sea ice thickness measurement from a theoretical perspective, and describe the general characteristics of the field data. In section III, we provide two measurement schemes termed as the fixed and the scaled radial sweep methods to obtain the field dataset. We also describe the deep learning model which learns the thickness and inherent dispersion relation of sea ice from the field measurements. In section IV we presents the performance of the deep learning model to characterize sea ice, with a qualitative comparison between the two measurement schemes, and discuss some possible limitations and scope for improvement of the near field measurement method. Finally, the results and our findings are summarized in section V.

II. Background Theory

In this section, we present a mathematical and physical interpretation of the EM field response of an air-sea ice-seawater environment [22] and describe how the field responses are related to the characterization parameters. As shown in Fig. 1, we consider a Hertzian electric dipole as the source of EM radiation, and label air, sea ice and seawater as layers 0, 1 and 2 respectively. Each layer has a complex dielectric constant of $\epsilon_{c,i}$, which consists of a real polarization component ϵ_i and an imaginary loss component $\tan\delta_i$ through the following relation:

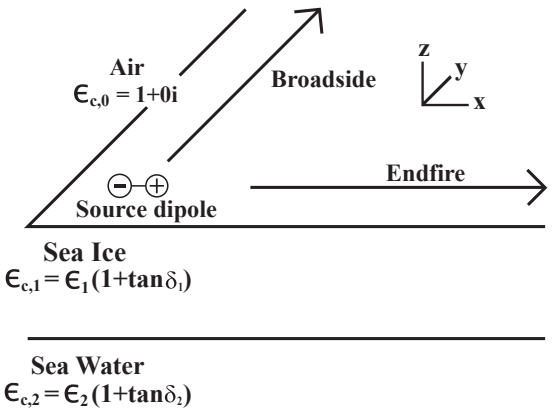

Fig. 1. Schematic diagram of the three layered air-sea ice-seawater environment, with stratification along the negative z axis

$$\epsilon_{c,i} = \epsilon_i(1 + \tan\delta_i), \text{where } i = 0, 1, 2$$

The EM fields depend on the "generalized planewave reflection coefficient" [6] of the three layered system, which in turn is a function of the thickness and the dielectric properties of the substrate (i.e. sea ice). The expression of the total reflection coefficient for the three layered system is [23]

$$\widetilde{R}_{0,1} = \frac{R_{0,1} + \widetilde{R}_{1,2}e^{2ik_{z,1}d}}{1 + R_{0,1}\widetilde{R}_{1,2}e^{2ik_{z,1}d}} \tag{1}$$

Here, the tilde superscript over the reflection coefficient denotes total generalized reflection, which considers the reflection from all the layers below. The reflection coefficients without tilde superscript indicates the "Fresnel reflection coefficient" between the two successive layers [24]. The propagation constant in each media is k_i, its component along the direction of stratification is $k_{z,i}$, for i= 1,2. the component tangential to the surface boundaries is k_t, and d is the thickness of sea ice. Dipole sources excite spherical waves, which can be decomposed into a tangential cylindrical wave component [25] and a planewave component along the direction of the stratification. Therefore, $k_t = k_\rho$, [23] and $k_i = \sqrt{k_\rho^2 + k_{z,i}^2}$. Throughout the paper, we have chosen an $e^{-j\omega t}$ time dependence, and therefore for choosing the appropriate square roots in all the following equations, we have taken the value which has a positive real and imaginary component to satisfy the radiation condition. For the source medium (air or medium 0), we omit the i subscripts from the propagation components to avoid congestion in the field expressions. That is, in the source region, the propagation

constant and the component along stratification are k and k_z respectively.

If we represent the term $2ik_{z,1}d$ in (1) in the angular representation [23], we can write assuming $|\epsilon_{c,1}| >> 1$:

$$2ik_{z,1}d = 2id\sqrt{k_1^2 - k_\rho^2} = \frac{4\pi id}{\lambda}\sqrt{\epsilon_{c,1} - \sin^2\theta}$$
$$\approx \frac{4\pi id}{\lambda}\sqrt{\epsilon_{c,1}} = g(\sqrt{\epsilon_{c,1}}d)$$

where, $\theta = \text{atan}\frac{k_\rho}{k_z}$ is the angle of incidence, which can be either real of complex. The reflection coefficient R can be either TE or TM mode. However, irrespective of the mode, since the ground is highly conductive, the bottom layer will always have reflection coefficient $R_{1,2} \approx \widetilde{R_{1,2}} \approx \pm 1 = e^{\pm i\pi}$. Now, for TM case, the expression of the Fresnel reflection coefficient between medium 0 and 1 (air and sea ice) is:

$$R_{0,1}^{TM} = \frac{\epsilon_{c,1}k_z - \epsilon_0 k_{z,1}}{\epsilon_{c,1}k_z + \epsilon_0 k_{z,1}}$$
$$= \frac{\epsilon_{c,1}\sqrt{\epsilon_0 - \sin^2\theta} - \epsilon_0\sqrt{\epsilon_{c,1} - \sin^2\theta}}{\epsilon_{c,1}\sqrt{\epsilon_0 - \sin^2\theta} + \epsilon_0\sqrt{\epsilon_{c,1} - \sin^2\theta}}$$
$$= \frac{\epsilon_{c,1}\cos\theta - \sqrt{\epsilon_{c,1} - \sin^2\theta}}{\epsilon_{c,1}\cos\theta + \sqrt{\epsilon_{c,1} - \sin^2\theta}}$$
$$= f_1(\sqrt{\epsilon_{c,1}}) \tag{2}$$

and, for TE waves:

$$R_{0,1}^{TE} = \frac{\mu_1 k_z - \mu_0 k_{z,1}}{\mu_1 k_z + \mu_0 k_{z,1}}$$
$$= \frac{\cos\theta - \sqrt{\epsilon_{c,1} - \sin^2\theta}}{\cos\theta + \sqrt{\epsilon_{c,1} - \sin^2\theta}}$$
$$= f_2(\sqrt{\epsilon_{c,1}}) \tag{3}$$

$$\widetilde{R_{0,1}} = \frac{f_j(\sqrt{\epsilon_{c,1}}) + e^{g(\sqrt{\epsilon_{c,1}}d)\pm i\pi}}{1 + f_j(\sqrt{\epsilon_{c,1}})e^{g(\sqrt{\epsilon_{c,1}}d)\pm i\pi}} \tag{4}$$

From (4), it is evident that both TM and TE reflection coefficients are functions of medium thickness and the dielectric property. Comparing (2) and (3) with (4), we also find that the TM reflection is a strong function of both $\epsilon_{c,1}$ and d, and TE reflection is a weaker function of $\epsilon_{c,1}$ but a strong function of d. The idea is, we excite a source which has both TM and TE component, then extract one TE field (a strong function of d) and a TM field (a strong function of ϵ_1 and d), and use them to estimate both the unknown parameters from the measurements. The choice of using a horizontal source dipole therefore is the convenient choice as it excites both field modes.

Even though the mathematical reasoning is plausible, there underlies some difficulties in simultaneously estimating the thickness and dielectric properties. Since the dielectric constant and thickness appear as a product term $(\sqrt{\epsilon_{c,1}}d)$ in (4), an error in measuring thickness should contribute to the erroneous estimation of dielectric constant to a certain degree, and vice versa. Furthermore, the complex and non linear nature of $\epsilon_{c,1}$ with frequency, makes the task of estimating the parameter more challenging.

We have chosen the frequency of operation in the MHz range as sea ice works as a partially transparent medium at this frequency range. The feasibility of the whole method depends on the fact that the air-sea ice interface will produce a partial and the sea ice-seawater interface will produce a total reflection; the combination of which will suppress the source field and provide information on the medium characteristics. The choice of the MHz frequency is convenient for two reasons.

- For lower frequencies, sea ice bulks have a very large dielectric constant [10], [11], [14], which results in almost total reflection from the top interface, and very few waves will leak through the bulk, which will result in a very low resolution in measurement performance.
- As sea ice bulk has a moderately high dielectric loss, a higher frequency would mean a larger propagation loss. Hence, the penetrating waves will attenuate very quickly inside the sea ice bulk before reflecting back to the receiver, and therefore there would be no information of the depth of sea ice.

Before divulging into the methodology section, we provide a physical interpretation of the variation of field magnitudes with changing thickness and dielectric constant of the sea ice. Since the bottom seawater layer is highly conductive, it will reflect almost all the waves from the sea ice-seawater interface (ray 1) as shown in Fig. 2. Another wave reflection will come from the air-sea ice interference (ray 2). With respect to the source, both of these reflected waves are in opposite phase, and will always try to cancel the source ray in the subwavelength or near field region. Hence the magnitude of the total fields will be lower. The more opposite in the phase the combined ray 1 and 2 are with respect to the source, the lower will be the total field response.

A. Relation with thickness d

When the thickness is low, ray 1 will travel less path from the bottom interface to the receiver point, therefore at the receiver, ray 1 will be more "out of phase" to the source, which will suppress the source field more, and the total field will be lower. When the thickness is large, ray 1 will travel a longer path, and therefore will be less "out of phase" compared to the source. In addition, the propagation inside a lossy sea ice bulk will degrade the magnitude of the reflected waves to some extent. This will result in a much weaker reflected wave opposing the phase of the source, and the cancellation will be smaller. So the total field response will be larger at large thickness values of sea ice and smaller

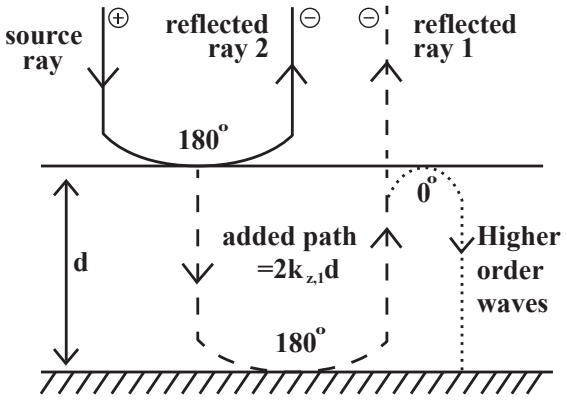

Fig. 2. Physical interpretation of the variation of field magnitudes with changing thickness and dielectric constant of the lossy substrate.

for small thickness values of sea ice. As shown in Fig. 3a, this effect is more pronounced with the TE waves, which strongly depend on the thickness.

B. Relation with ϵ_1 and $tan\delta_1$

The larger the value of epsilon, the larger will be the reflection from the top interface (ray 2) and there will be more reflected waves cancelling out the source. So the total field response will be lower. In the same token, the lower the value of epsilon, the lower the reflection from the top interface and the larger the response of the field values. Addition of the medium loss will contribute not just to the reflection magnitude, but also to the phase of the top surface of the reflection coefficient, which will effect the reflection characteristics. In general, the higher the loss tangent, the more the reflection from the top surface, and the lower the total field will be. The phenomenon is more prominent in the TM reflections, which is a strong function of both the thickness and the dielectric properties of the sea ice bulk (see Fig. 3b).

III. Methodology

In this section we will discuss the method by which the thickness and the dielectric properties of sea ice can be estimated from the dipole radiated field values. As stated earlier, we will consider the air-sea ice- seawater system as a planar, three layered stratified system, and the frequency will be in the MHz range. We choose to solve the inverse problem of estimating the thickness and the dielectric properties using a deep learning model, which needs sufficient data to train and later to test the performance of the model. The training data is generated using both an analytical method and a finite element (FEM) simulation. We use analytical data to describe the feasibility of solving such an inverse problem from a theoretical perspective. In addition, due to the ease of computation, we are also able to generate an enormous amount of data using analytical method, so that the model will always be very well trained and the results would be

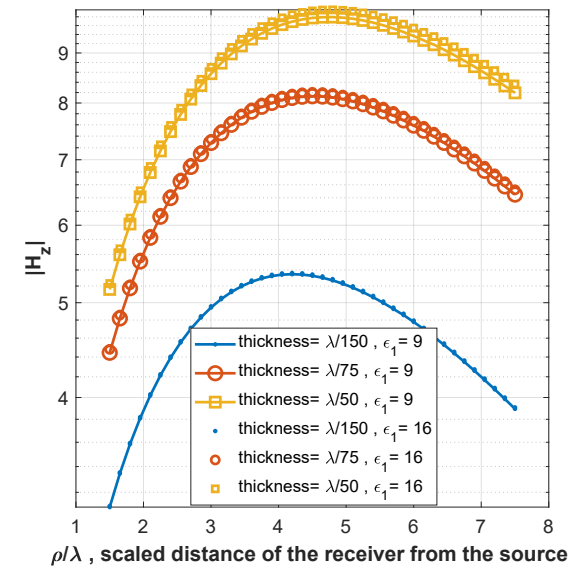

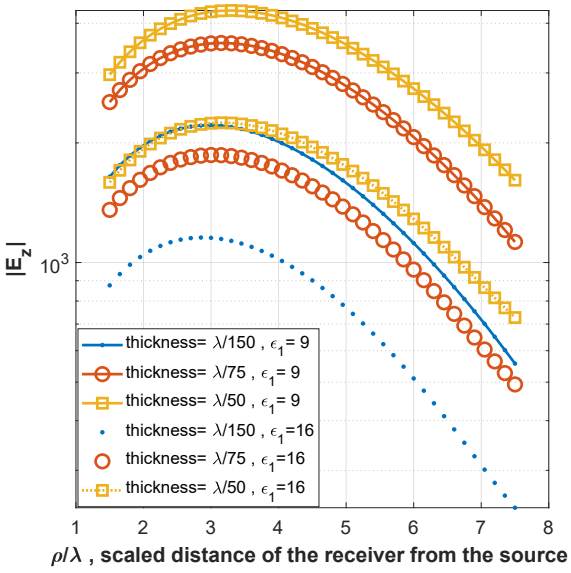

Fig. 3. Variation of TE and TM mode fields with radial distance of the receiver from the source for different thickness and dielectric constants of the substrate. The solid lines are for $\epsilon_1 = 9$, and the dotted lines are for $\epsilon_1 = 16$. Fig. (a) shows strong dependency of H_z on thickness and Fig. (b) shows strong dependency of E_z on both thickness and dielectric constant.

clearly interpreted and understood. On the other hand, FEM simulation data is more representative of practically acquired data, which should be much less in quantity and the error propagation can be thought of as an error in measurement schemes. The FEM simulation environment is generated using COMSOL Multiphysics [26], a physics simulation software. Due to the relatively large computation time, the amount of generated data is much much less than those in the analytical methods, and therefore the model is likely to be overfitted on the training data. For the FEM modeling,

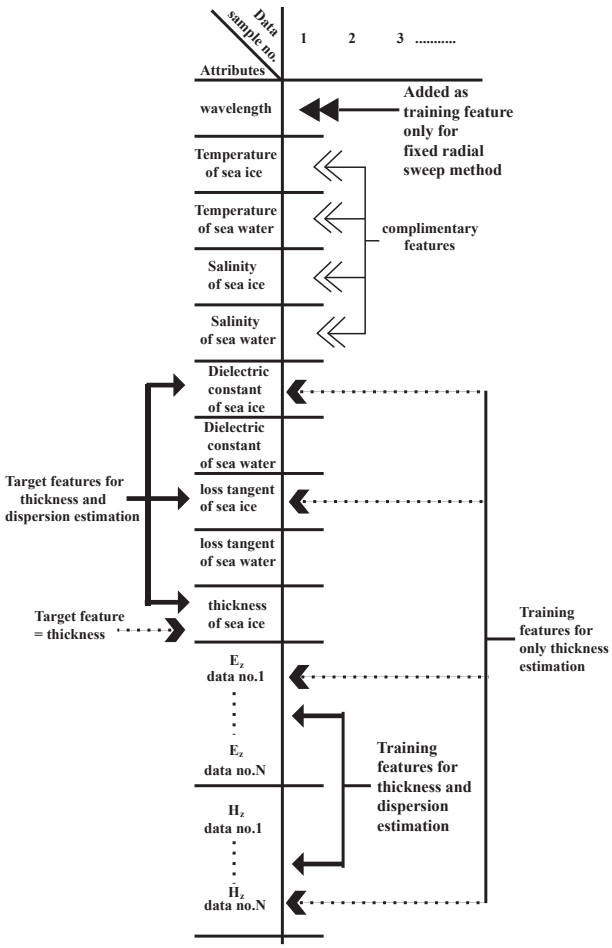

Fig. 4. Attributes of the data samples used to solve the inverse problem. The left arrows point to the training features, and the right arrows point to the target values. The solid arrows represent the attributes used to estimate both dispersion and thickness of sea ice. The dotted arrows correspond to attributes when estimating thickness of sea ice only. The four double arrows pointed to the left denote the complimentary features, which are neither used for training nor as targets. The wavelength is used as an additional training feature for the fixed radial sweep method. N is the number of data along the measurement direction for the choice of radial sweep.

we chose the meshing to be relatively coarse, just enough so as the integrity of the data is maintained, therefore ensuring a faster computation as a tradeoff, and generate a reasonable amount of data.

We describe the method of solving the inverse problem of sea ice thickness in three steps. First, we will define the three layered air- sea ice - sea water environment, then we will generated field data for training and testing over a band of frequencies, and finally we will use the dataset to train a deep learning network capable of solving the inverse problem of simultaneous estimation of the thickness and dispersion relations.

A. Modelling of the three layered system

The top layer (air) is the simplest to model, with a constant dielectric constant of $\epsilon_0 = 1$, and loss tangent $\tan\delta_0 = 0$. For modeling of the sea ice bulk, we have used the dispersion curves presented in [12]. The dispersion of sea ice is a direct function of temperature, frequency and salinity of the ice sample. Due to the exponential and monotonic dispersion relation in the low MHz ranges, we have used linear interpolation to estimate the dielectric constants at different temperature and salinity values.

The dielectric modelling of seawater is available in [9], [27], where the dispersion of the sea water sample is fitted into a debye model as follows:

$$\epsilon_{c,2} = \epsilon_{inf} + \frac{\epsilon_s - \epsilon_{inf}}{1 + i\omega\tau_s} - \frac{i\sigma_s}{\omega\epsilon_0}; \tag{5}$$

Here,

$$\begin{aligned}
\epsilon_{ref} &= 87.134 - 1.949\times10^{-1}T - 1.276\times10^{-2}T^2 \\
&\quad + 2.491\times10^{-4}T^3 \\
\sigma_{ref} &= S(0.182521 - 1.46192\times10^{-3}S + 2.09324 \\
&\quad \times10^{-5}S^2 - 1.28205\times10^{-7}S^3) \\
\tau_{ref} &= 1.768\times10^{-11} - 6.086\times10^{-13}T \\
&\quad + 1.104\times10^{-14}T^2 - 8.111\times10^{-17}T^3 \\
\alpha &= 1 + 1.613\times10^{-5}ST - 3.656\times10^{-3}S \\
&\quad + 3.210\times10^{-5}S^2 - 4.232\times10^{-7}S^3 \\
\epsilon_s &= \epsilon_{ref}\alpha \\
\Delta &= 25 - T \\
\beta &= 2.033\times10^{-2} + 1.266\times10^{-4}\Delta + 2.464\times10^{-6}\Delta^2 \\
&\quad - S(1.849\times10^{-5} - 2.551\times10^{-7}\Delta + 2.551\times10^{-2}\Delta^2) \\
\sigma_s &= \sigma_{ref}\exp(-\Delta\beta) \\
\gamma &= 1 + 2.282\times10^{-5}ST - 7.638\times10^{-4}S \\
&\quad - 7.760\times10^{-6}S^2 + 1.105\times10^{-8}S^3 \\
\tau_s &= \tau_{ref}\gamma \\
\epsilon_{inf} &= 4.9
\end{aligned}$$

where T is the temperature in degree Celsius, and S is the salinity in ppt (parts per thousand).

B. Description of the environment and dataset:

For the hypothetical three layered air-sea ice- sea water system, we assume a horizontal electric dipole as the excitation source. The source is placed on the sea ice surface. To measure field components, we choose the z component of the decoupled E and H fields as the necessary TM and TE field data. E_z will be measured along the endfire [28] direction, and H_z will be measured along the broadside direction. The expressions of the two fields are given below [23]:

$$\vec{E_z}^{TM} = \int_{-\infty}^{\infty} i\frac{Il}{8\pi\omega\epsilon_0}\left[k_\rho^2\left(1-\widetilde{R}_{0,1}^{TM}\right)e^{ik_z z}H_1^{(1)}(k_\rho\rho)\cos\phi\right]dk_\rho \tag{6}$$

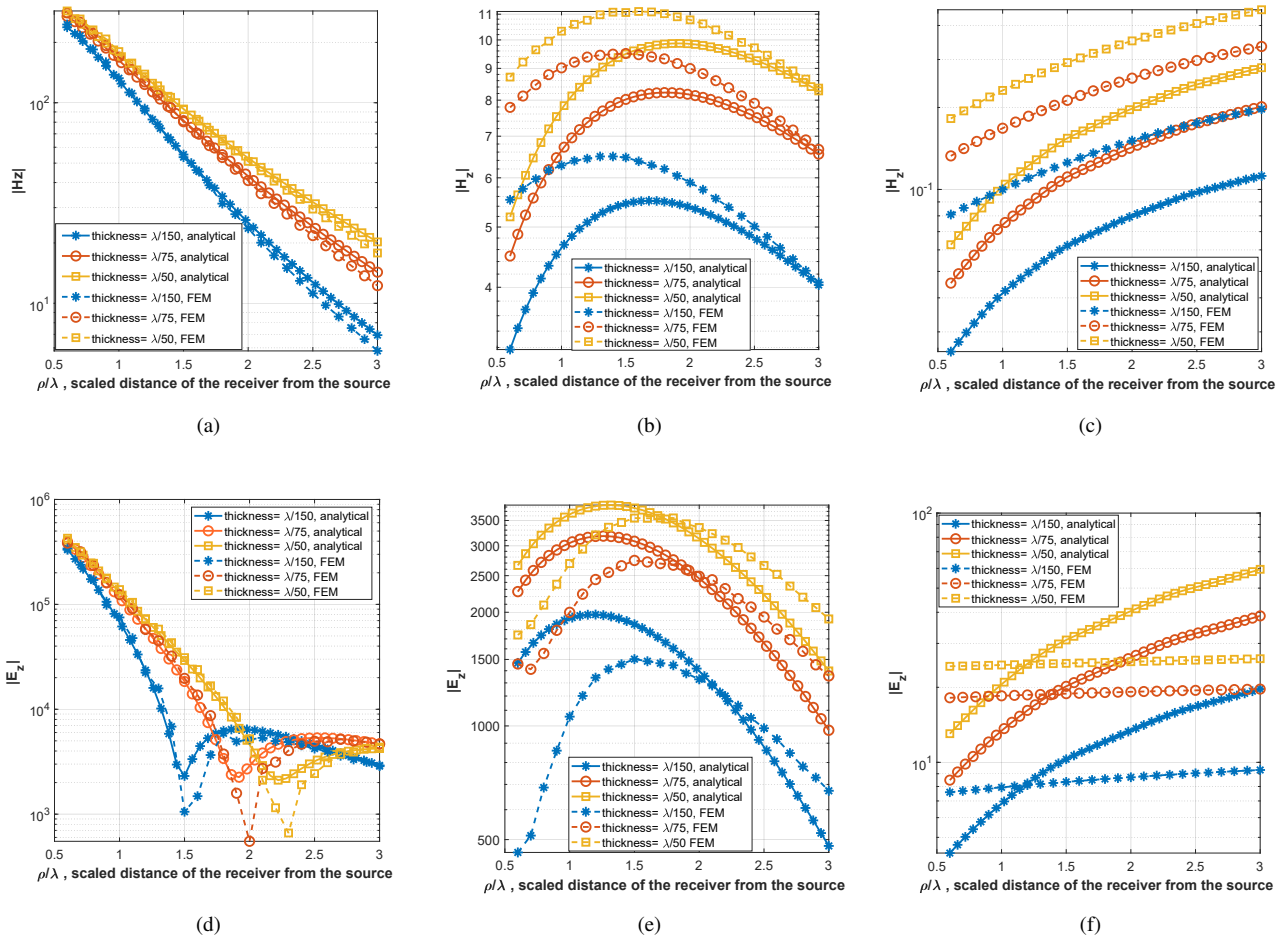

Fig. 5. The E_z and H_z field response with variation of the receiver height. Field values are obtained using mathematical computation and FEM simulation. We have used $f = 5$ MHz, $\epsilon_0 = 1, \epsilon_{c,1} = 10(1 + 0.5i), \epsilon_{c,2} \approx i\infty$, $z = 0.01\lambda$ in Figs. (a) and (d), $z = 0.05\lambda$ in Figs. (b) and (e), $z = 0.2\lambda$ in Figs. (c) and (f).

$$\vec{H}_z^{\,TE} = \int_{-\infty}^{\infty} i\frac{Il}{8\pi}\left[\frac{k_\rho^2}{k_z}\left(1+\widetilde{R}_{0,1}^{TE}\right)e^{ik_z z}H_1^{(1)}\left(k_\rho\rho\right)\sin\phi\right]dk_\rho \tag{7}$$

Here, ρ is the radial distance from the source to the receiver, ϕ is the azimuth angle which defines the radiation direction ($\phi = 0$ is the endfire direction and $\phi = \pi/2$ is the broadside direction. I and l are the driving current and arm length of the dipole respectively, $\omega = 2\pi f$ is the frequency of operation. k_ρ is the tangential component of the dipole radiation, $k_z = k_{z,0}$ is the propagation component along the direction of stratification, and z is the height of the receiver. We refer to [6], [23] for the description of each of the terms and will not elaborate in this article.

The dataset consist of "train features" and "target values". The train features include the electric and magnetic field values at defined receiver distance from the source, and the target values are the concerned thickness and dielectric properties of the sea ice bulk. There are also some "complimentary features" such as the temperature and salinities of the sea ice and sea water media; which are required to generate the dielectric properties of the three layered systems but not used to train the deep learning models. The arrangement of the dataset in tabular form is presented in Fig. 4.

The training features are generated over a range of frequencies as shown in Table I so that the model can learn the frequency dependent dielectric and loss tangent properties. Furthermore, it allows us to check the performance of the model when the test frequency is inside and outside the training frequency bands; therefore we can evaluate the frequency adaptation of the trained model. If the performance of the model is acceptable outside the training bands, we can use a narrow band training data and apply the model over a wide range of frequencies. On the other hand, if the test features work only inside the training range, we need to train a larger model using a wide band training data.

First, to generate the data, we needed to determine the height of the receiver and the spatial range across which the receiver dipole will be swept to capture the field data. We followed two approaches,

TABLE I
RANGES OF EACH PARAMETER TO GENERATE DIFFERENT AIR-SEA ICE-SEA WATER ENVIRONMENTS. $[a, b]$ IS A CLOSE INTERVAL RANGING FROM a TO b.

Ranges of data for field generation	Fixed		scaled	
	Anlaytical	FEM	Anlaytical	FEM
Frequency (MHz)	[2,5]	[2,5]	[2,5]	[2,5]
Temperature of sea ice (° C)	[-35,-10]	[-35,-15]	[-35,-10]	[-35,-15]
Temperature of sea water (° C)	[2,8]	[2,5]	[2,8]	[2,5]
Salinity of sea ice (ppm)	[2.2,5.16]	[2.2,5.16]	[2.2,5.16]	[2.2,5.16]
Salinity of sea water (ppm)	[6.4,25.2]	[6.4,25.2]	[6.4,25.2]	[6.4,25.2]
Thickness of sea ice (d) (m)	[0.5, 7]	[0.5, 7]	-	-
d/λ of sea ice	-	-	[0.05,0.1]	[0.05,0.1]
Receiver height (z) (m)	2	2	-	-
z/λ height	-	-	0.05	0.05
Receiver distance from the source (ρ) (m)	[3,15]	[3,15]	-	-
ρ/λ distance from the source	-	-	[0.01,0.05]	[0.01,0.05]
Number of measurement data point	122	42	68	22
Number of data samples	142740	2688	315120	8568

- In the first method, the height of the receiver and the spatial range of measurement with respect to the source dipole remains constant. We term this method of measurement as "Fixed radial Sweep" of the receiver. The thickness of the sea ice layer is assumed to be within 1m to 6m, which is the typical thickness of the ice samples in the polar region [22]. We have chosen the receiver height to be 2m, and the sweep distance of the receiver is set from 3m to 15 m. Both of them are empirical choices. We have also chosen the wavelength (λ) of the excitation source as one of the training features for fixed radial sweep, as adding wavelength as an additional feature improves the performance of the deep learning network.
- In the second approach, measurement distance and the receiver height were scaled with respect to the wavelength. We term the method of measurement as "Scaled radial sweep" of the receiver. The receiver distance from the source was varied from 0.01 λ to 0.05 λ, and the height was fixed at 0.05 λ for each operating frequency. Although the choice of the receiver height was empirical, we have noted that if the receiver is placed too close to the sea ice surface, the field magnitudes diminish very quickly with increased receiver distance (see Figs. 5a and 5d). A slightly larger height of the receiver tend to keep the field magnitude uniform with increased receiver distance (see Figs. 5b and 5e); however, an arbitrary large height will increase the source receiver distance too much, which causes the field signals to be very small,(see Figs. 5c and 5f). From these observation of field patterns at different heights, we chose a value of z= 0.05 λ, for the dataset generation.

  For the scaled radial sweep method, the wavelength is removed from the training features, as all the parameters are scaled with respect to wavelength and the structures are frequency independent, the wavelength would add no additional information. We also note that removing wavelength from the training features slightly improve the performance of the training model.

When we try to measure the thickness and dispersion

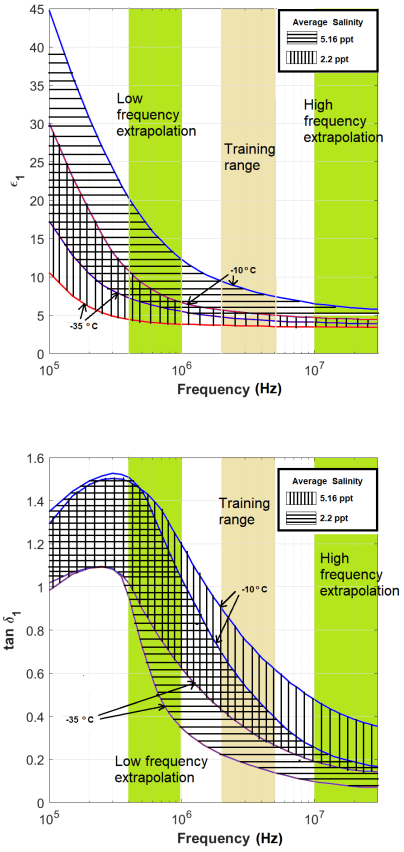

Fig. 6. Extrapolation of the dispersion curves of sea ice outside the training bounds: (a) extrapolation of dielectric constant (b) extrapolation of the loss tangent. The dispersion curves are taken directly from [12].

curves beyond the training frequency range, we expect that the scaled radial sweep method would perform better than the fixed sweep method. Because the former method enables us to get an approximately wavelength-independent representation of the field values, where the receiver distance, height and the measured thickness is scaled to the wavelength, and the only frequency-dependent variant is the dispersion rela-

tion embedded in the reflection coefficients (the derivation is provided in Appendix A). The concept is further explained in Fig. 6, where the training frequency range and extrapolated test frequency ranges are specified on the dispersion curves obtained from experimental data. The curves are somewhat exponential and monotonically decreasing in all the three specified ranges and therefore, the model trained on the middle range should be able to extrapolate the prediction outside the training frequency boundary.

C. Description of the deep learning model:

As for the deep learning model, we have chosen a simple three layered multilayer perceptron (MLP) for mapping the input features into target values. For the fixed radial sweep, the input layer consist of the wavelength and the magnitude of the field values. For the scaled radial sweep, only the field magnitudes are used in the input layer. The field data are normalized using standard Z-score normalization. When we try to estimate both the thickness and the dielectric properties, the output layer included the ϵ_1, $tan\delta_1$ and the thickness values of the sea ice models. When we examined the performance of the model to estimate the thickness only, the ϵ_1 and $tan\delta_1$ values are used as input features and the thickness of the sea ice is the only output value.

The structure of the deep learning layers is shown in Fig. 7. The intermediate layers are a series of three fully connected layers, with 512, 1024 and 2048 nodes respectively at each layer. Each layer is non linearized using the ReLu activation. The final layer, or the output layer has no activation function as the outputs are regressive. Since the inverse problem of solving the thickness and the dielectric constants from the field data is a regression problem, we use the mean squared error (MSE) as the main loss function to update the parameters of the model. As for the optimizer, Adam optimizer has been defined, with an initial learning rate of 0.001. The training data is divided into an 8:2 train to validation set, and the batch size is set to 16. In order to tackle overfitting, the learning rate is reduced at each plateau, and the epoch count stopped after sufficient epoch count failed to improve the validation loss.

IV. RESULTS

In this section, we present the performance of the deep learning network to solve the inverse problem of estimating the thickness and dielectric properties of sea ice on different test datasets. For the performance evaluation, we have defined the mean absolute percentage error (MAPE) as the evaluation metric, which is given as follows:

$$MAPE = \frac{1}{I}\sum_{i}\left|\frac{actual\_value(i) - predicted\_value(i)}{actual\_value(i)}\right| \times 100\%$$

Where, $I = \sum i$

We first observe that the model learns very well with the analytical dataset. Fig. 8a and 8b show the training and validation loss curves for this dataset. We see that the validation loss is quite low for both fixed and scaled radial sweeps, and there is no sign of overfitting. To the contrary, training with the FEM dataset results in higher validation loss, as can be seen in Fig. 8a and 8d. There is some overfitting to the training dataset due to the small amount of FEM data.

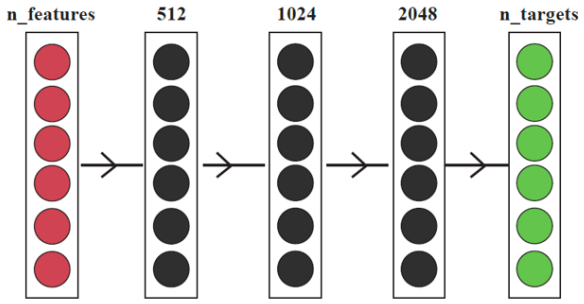

(a)

Measurement Method	Estimation parameters	n_features	n_targets
Fixed radial sweep	$\epsilon_{c,1}$, d	$1 + 2m$	3
	d	$3 + 2m$	1
Scaled radial sweep	$\epsilon_{c,1}$, d	$2p$	3
	d	$2 + 2p$	1

(b)

Fig. 7. (a) Architecture of the deep learning model for solving the inverse problem. (b) The number of input features and output values for different measurement methods and estimation parameters. Here, m is the number of electric/magnetic field measurement points for fixed radial sweep and p is the number of electric/magnetic field measurement points for scaled radial sweep.

A. simultaneous characterization of sea ice

Now we present the performance of our model for simultaneous characterization of sea ice using fixed and scaled radial sweep methods. We also show whether a set of training data with a defined frequency band can be used to interpolate at different measurement frequencies.

1) Fixed radial sweep: Fig. 9a describes the efficacy of the model to solve the inverse problem for fixed radial sweep measurements. From the analytical test sets, we can see that when the test dataset's frequency is in the frequency range of the training set, the percentage error of ϵ_1 is always less than 2%, the $\tan\delta_1$ error is less than 10% , and the thickness error is less than 5%. This suggests that the simultaneous estimation of all three parameters is indeed possible, and the model is capable of showing a high degree of accuracy. However, for this method, if the measurement frequency is even slightly outside the training range, performance of the model degrades very rapidly. The thickness parameters deteriorates the fastest, while ϵ_1 and $tan\delta_1$ degrades more gradually. Therefore, it can be said that the fixed radial sweep measurement is not capable of frequency domain

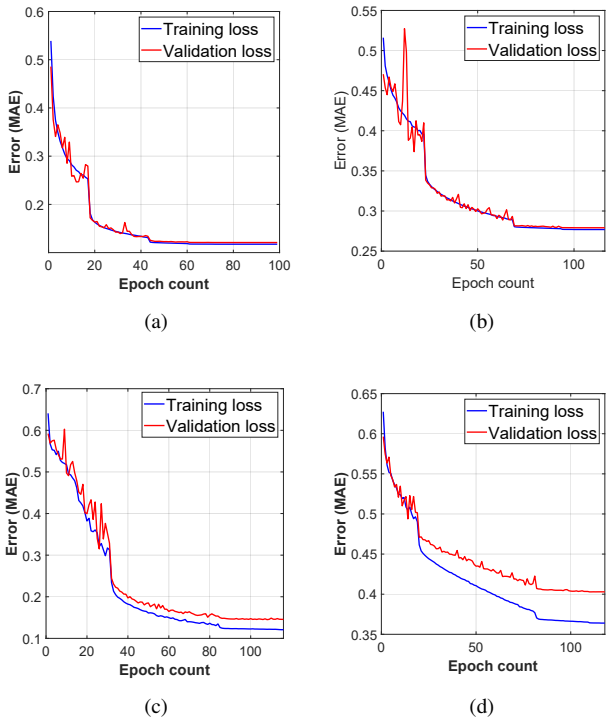

Fig. 8. Training and validation loss curves of the deep learning model for different methods of training. (a) fixed radial sweep with analytical data, (b) scaled radial sweep with analytical data (c) fixed radial sweep using FEM model, (d) scaled radial sweep using FEM model

adaptation, but a very viable method to solve the inverse problem provided the measurement data is within the training range.

2) Scaled radial sweep: Fig. 9b shows the performance of the model when we take a scaled approach to solve the problem. We notice, when the measurement frequency is inside the training limits, ϵ_1, $tan\delta_1$ and d errors for analytical dataset is less than 1%, which is a significant improvement compared to the fixed radial sweep. The performance degradation for test frequencies outside the training limits is also gradual, and even for frequencies as high and low by a factor of 5, we see that the estimation error is less than 10% for ϵ_1 and $tan\delta_1$, and less than 20% for d.

Though the scaled radial sweep performs better than the fixed radial sweep, the gradual increase of error indicates that the model is not capable of completely learning the dispersion relations of the sea ice and sea water models outside the training limits. The intertwined relation between the thickness and the dielectric properties as mentioned in Section II may cause an estimation error.

On the contrary, the fixed radial sweep fails even when the test frequency is slightly outside the training frequency range. This is because, if we keep the receiver height fixed, then that would imply different $\frac{z}{\lambda}$ ratio for each frequency of measurement. This results in completely different patterns of field magnitudes (see Fig. 6) which is difficult to learn by the model.

Comparing the analytical results with the FEM estimations, we do see some degradation of quality for the latter. Specially, for the scaled sweep method, the improvement in performance is not so obvious. This can be attributed to insufficient amount of FEM data used for the training, which resulted in a quick overfitting of the model, which was not the case for estimation using the analytical measurements.

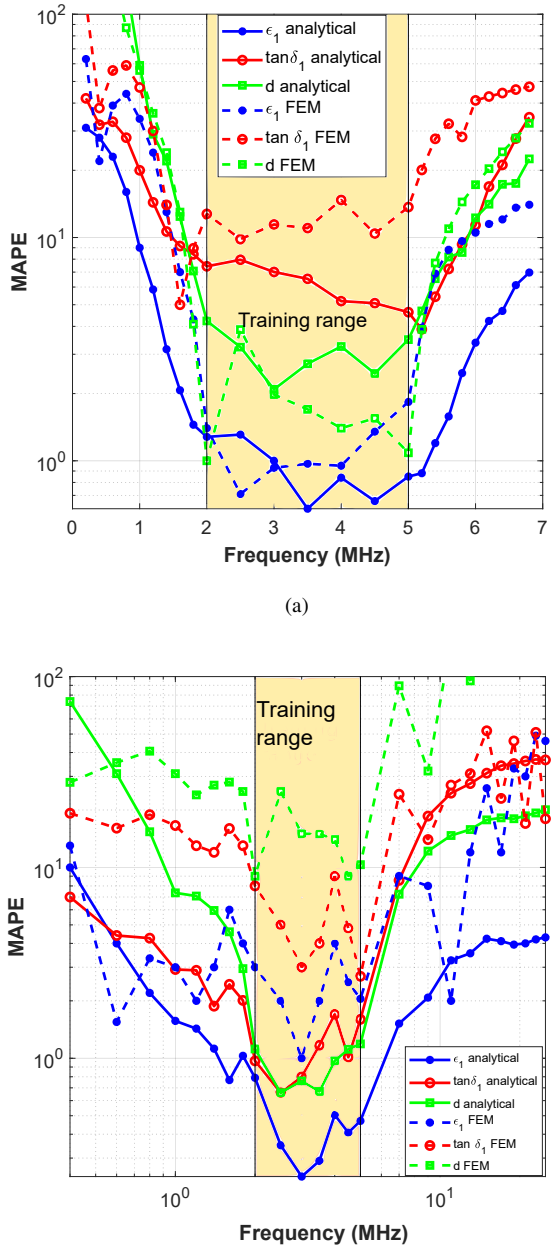

Fig. 9. Estimation error of ϵ_1, $tan\delta_1$ and d for the test dataset at different measurement frequencies: (a) fixed radial sweep (b) scaled radial sweep.

B. Estimation of sea ice thickness

Finally, we have chosen to test the performance of our deep neural network in determining the thickness only, assuming ϵ_1 and $tan\delta_1$ are known a priori. In this case, the ϵ_1

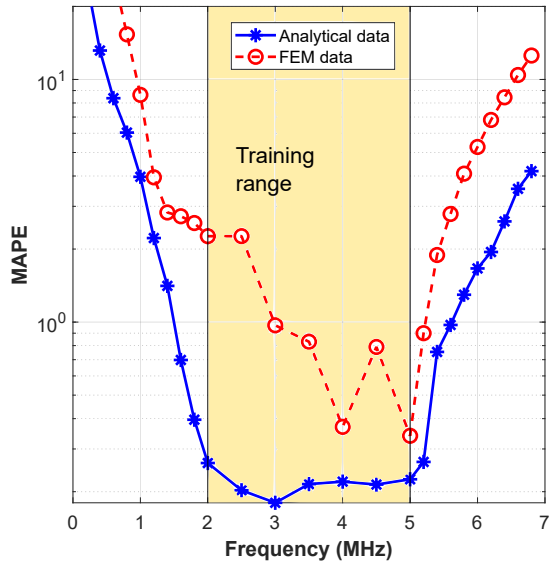

(a)

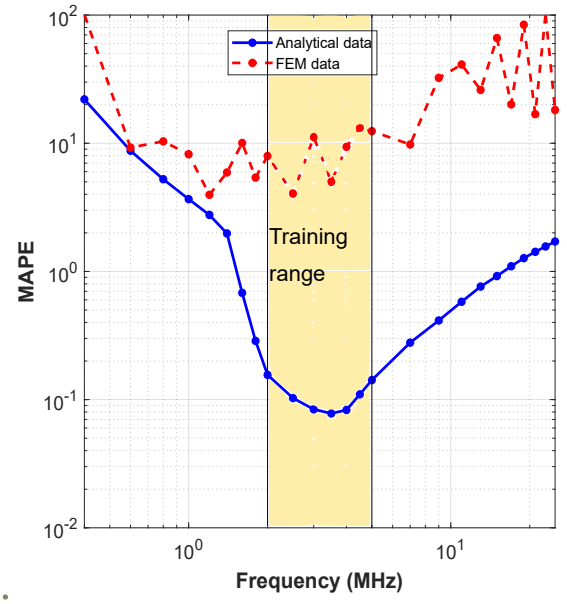

(b)

Fig. 10. Estimation error of determining the sea ice thickness using a priori dielectric information: (a) fixed radial sweep (b) scaled radial sweep.

and $tan\delta_1$ values are passed to the deep learning network as training features, and the thickness d remains the only target to be estimated. Now the thickness measurement error, as shown in Fig. 10, has improved drastically over all the ranges of test frequency for both the fixed and the variable sweep methods. We can see that the error is close to 0% inside the training frequency range, and it is less than 20% outside the training frequency range. However, a noticeable error still persists when FEM data is considered.

V. Conclusion

In this work, we have examined multiple schemes of thickness and dielectric estimation of sea ice over seawater. Deep learning models trained on both analytical and FEM data show good measurement accuracy, particularly when the thickness is determined as a sole parameter. For practical usecase and the most accurate evaluation of this method, extensive physical measurements and data acquisition will be necessary. While we believe that a thorough demonstration and the feasibility has been presented, there is also significant scope for improvements. Instead of using the "analytically efficient" dipole antennas, there is definite possibility of developing more complex antenna systems, which would radiate more along the stratification layers and capture stronger field responses. The one-dimensionality of the radial sweep does pose a strict practical limitation that the receiver height to wavelength ratio must always be nearly constant, and this practical aspect of the problem could/may be circumvented using more elaborate 2D and 3D mapping over multiple receiver location. Overall, this work provides the baseline methodology to simultaneously estimate the thickness and dispersion characteristics of sea ice, and the performance of the proposed method is already very encouraging. Branching out further research and undertaking steps for practical experiments would improve on this baseline, which is a part of further work.

Acknowledgment

This work has been supported by the Office of Naval Research Global, London, UK [grant N62909-19-1-2013] as part of the NICOP project "Non-invasive measurement of sea ice thickness using low frequency EM waves".

References

[1] A. P. Annan, "Radio Interferometry Depth Sounding: Part I-Theoretical Discussion," *Geophysics*, vol. 38, no. 3, pp. 557–580, Jun. 1973. [Online]. Available: https://doi.org/10.1190/1.1440360

[2] J. R. Rossiter, G. A. LaTorraca, A. P. Annan, D. W. Strangway, and G. Simmons, "Radio Interferometry Depth Sounding: Part II - Experimental Results," *Geophysics*, vol. 38, no. 3, pp. 581–599, Jun. 1973.

[3] L. Tsang, J. A. Kong, and G. Simmons, "Interference patterns of a horizontal electric dipole over layered dielectric media," *Journal of Geophysical Research (1896-1977)*, vol. 78, no. 17, pp. 3287–3300, Jun. 1973. [Online]. Available: https://agupubs.onlinelibrary.wiley.com/doi/abs/10.1029/JB078i017p03287

[4] W. C. Chew and J. A. Kong, "Electromagnetic field of a dipole on a two-layer Earth," *Geophysics*, vol. 46, no. 3, pp. 309–315, Mar. 1981.

[5] DaHan Liao and K. Sarabandi, "Near-earth wave propagation characteristics of electric dipole in presence of vegetation or snow layer," *IEEE Transactions on Antennas and Propagation*, vol. 53, no. 11, pp. 3747–3756, Nov 2005.

[6] M. S. Islam, S. Shafi, M. I. Hasan, and M. A. Haque, "Low frequency near field interferometry for characterization of lossy dielectric and an investigation on sea ice," *IEEE Transactions on Geoscience and Remote Sensing (Early Access)*, pp. 1–11, 2020.

[7] M. S. Islam, S. Shafi, and M. A. Haque, "Development of an experimental model of low frequency dipole radiation in the presence of multilayered structures," in *SoutheastCon 2021*. IEEE, 2021, pp. 1–6.

[8] ——, "Low-frequency electromagnetic characterization of layered media using deep neural network," in *2021 International Symposium on Antennas and Propagation (ISAP)*. IEEE, 2021, pp. 1–2.

[9] A. Stogryn, "Equations for calculating the dielectric constant of saline water (correspondence)," *IEEE transactions on microwave theory and Techniques*, vol. 19, no. 8, pp. 733–736, 1971.

[10] J. R. Addison, "Electrical properties of saline ice," *Journal of Applied Physics*, vol. 40, no. 8, pp. 3105–3114, 1969.

[11] A. Stogryn, "An analysis of the tensor dielectnc constant of sea ice at microwave frequencies," *IEEE transactions on geoscience and remote sensing*, no. 2, pp. 147–158, 1987.

[12] F. Wentworth and M. Cohn, "Electrical properties of sea ice at 0.1 to 30 mc/s," *J. Res. NBS*, vol. 68, pp. 681–691, 1964.

[13] S. Evans, "Dielectric properties of ice and snow–a review," *Journal of glaciology*, vol. 5, no. 42, pp. 773–792, 1965.

[14] S. Buchanan, M. Ingham, and G. Gouws, "The low frequency electrical properties of sea ice," *Journal of Applied Physics*, vol. 110, no. 7, p. 074908, 2011.

[15] M. Hallikainen and D. P. Winebrenner, "The physical basis for sea ice remote sensing," *Washington DC American Geophysical Union Geophysical Monograph Series*, vol. 68, pp. 29–46, 1992.

[16] B. Holt, P. Kanagaratnam, S. P. Gogineni, V. C. Ramasami, A. Mahoney, and V. Lytle, "Sea ice thickness measurements by ultrawideband penetrating radar: First results," *Cold Regions Science and Technology*, vol. 55, no. 1, pp. 33–46, 2009.

[17] R. L. Tilling, A. Ridout, and A. Shepherd, "Estimating arctic sea ice thickness and volume using cryosat-2 radar altimeter data," *Advances in Space Research*, vol. 62, no. 6, pp. 1203–1225, 2018, the CryoSat Satellite Altimetry Mission: Eight Years of Scientific Exploitation. [Online]. Available: https://www.sciencedirect.com/science/article/pii/S0273117717307901

[18] R. Lindsay and A. Schweiger, "Arctic sea ice thickness loss determined using subsurface, aircraft, and satellite observations," *The Cryosphere*, vol. 9, no. 1, pp. 269–283, 2015.

[19] E. Schanda, *Physical fundamentals of remote sensing*. Springer Science & Business Media, 2012.

[20] R. H. Bourke and R. P. Garrett, "Sea ice thickness distribution in the arctic ocean," *Cold Regions Science and Technology*, vol. 13, no. 3, pp. 259–280, 1987.

[21] H. Eicken, W. Tucker, and D. Perovich, "Indirect measurements of the mass balance of summer arctic sea ice with an electromagnetic induction technique," *Annals of Glaciology*, vol. 33, pp. 194–200, 2001.

[22] D. Thomas and G. Dieckmann, *Sea ice - 2nd Edition*. Wiley-Blackwell, 01 2010.

[23] W. Chew, *Waves and fields in inhomogeneous media*. Springer, 1990.

[24] D. K. Cheng *et al.*, *Field and wave electromagnetics*. Pearson Education India, 1989.

[25] J. R. Wait, A. Cullen, V. Fock, J. Wait, and H. Hagger, "Electromagnetic waves in stratified media," *Physics Today*, vol. 17, no. 4, p. 76, 1964.

[26] C. Inc., "Comsol," 2020. [Online]. Available: http://www.comsol.com/products/multiphysics/

[27] L. Klein and C. Swift, "An improved model for the dielectric constant of sea water at microwave frequencies," *IEEE transactions on antennas and propagation*, vol. 25, no. 1, pp. 104–111, 1977.

[28] C. A. Balanis, *Antenna theory: analysis and design*. John wiley & sons, 2015.

APPENDIX

A. Wavelength normalized representation of the field values

Let, the receiver distance, height and thickness of the sea ice, are expressed as a constant scaling factors of wavelength, i.e. $\rho = c_1\lambda$, $z = c_2\lambda$ and $d = c_3\lambda$. Since the wave propagation constant, $k = \frac{2\pi}{\lambda}$, the tangential component, $k_\rho = \frac{2\pi}{\lambda} sin\theta$, and the component along propagation $k_z = \frac{2\pi}{\lambda} cos\theta$, from section II we can write $k_\rho\rho = 2\pi c_1 \sin\theta$, $k_z z = 2\pi c_2 \cos\theta$ and $g(\sqrt{\epsilon_{c,1}}d) = 2ik_{z,1}d = 4i\pi c_3\sqrt{\epsilon_{c,1}}$. Substituting these values to equation (4) we get:

$$\widetilde{R_{0,1}} = \frac{f_j(\sqrt{\epsilon_{c,1}}) + e^{4i\pi c_3\sqrt{\epsilon_{c,1}} \pm i\pi}}{1 + f_j(\sqrt{\epsilon_{c,1}})e^{4i\pi c_3\sqrt{\epsilon_{c,1}} \pm i\pi}} = \widetilde{R_j}(\epsilon_{c,1}, c_3) \quad (8)$$

with j= 1, 2 representing TM or TE reflection. Considering free space (where $\omega = kc$, c being the speed of wave propagation) and modifying (6) we find:

$$\begin{aligned} E_z^{TM} &= K_1 \int_{-\infty}^{\infty} (\frac{2\pi}{\lambda})^2 sin^2\theta (1 - \widetilde{R_1}(\epsilon_{c,1}, c_3)) e^{2\pi i c_2 cos\theta} \\ &\quad \cdot H_1^1(2\pi c_1 \sin\theta)\cos\phi\cos\theta d\theta \\ &\propto \frac{1}{\lambda^2}\int_{-\infty}^{\infty} (1 - \widetilde{R_1}(\epsilon_{c,1}, c_3)) e^{2\pi i c_2 \cos\theta} H_1^1(2\pi c_1 \sin\theta) \\ &\quad \cdot \sin^2\theta\cos\theta\cos\phi d\theta \end{aligned} \quad (9)$$

where, $K_1 = \frac{iIl}{8\pi c\epsilon_0}$. Since c_1, c_2 and c_3 are all constant terms and the only frequency-dependent term is $\widetilde{R_1}(\epsilon_{c,1}, c_3)$, the values of E_z^{TM} during the radial sweep become weakly dependent on frequency. Similary, it can be shown from (7) that the normalized H_z^{TE} is also weakly dependent on the frequency:

$$\begin{aligned} H_z^{TE} &\propto \frac{1}{\lambda^2}\int_{-\infty}^{\infty} (1 + \widetilde{R_2}(\epsilon_{c,1}, c_3)) e^{2\pi i c_2 \cos\theta} H_1^1(2\pi c_1 \sin\theta) \\ &\quad \cdot \sin^2\theta\cos\theta\sin\phi d\theta \end{aligned} \quad (10)$$

REPORT DOCUMENTATION PAGE

Form Approved
OMB No. 0704-0188

1. REPORT DATE *(DD-MM-YYYY)*	2. REPORT TYPE	3. DATES COVERED *(From - To)*
30-06-2022	Final Research Performance Progress Report	Dec 3, 2018 - Jun 30, 2022

4. TITLE AND SUBTITLE
Non-invasive measurement of sea ice thickness using low frequency EM waves

5a. CONTRACT NUMBER
N62909-19-1-2013

5b. GRANT NUMBER
GRANT12608455

5c. PROGRAM ELEMENT NUMBER
N/A

6. AUTHOR(S)
Haque, Mohammad Ariful;
Islam, M. Shifatul;
Shafi, Sadman;
Hasan, Md. Imrul

5d. PROJECT NUMBER
N/A

5e. TASK NUMBER
N/A

5f. WORK UNIT NUMBER
N/A

7. PERFORMING ORGANIZATION NAME(S) AND ADDRESS(ES)
Anyeshan Limited
206/A, Tejgaon Industrial Area, Dhaka-1208
Bangladesh

8. PERFORMING ORGANIZATION REPORT NUMBER
N/A

9. SPONSORING/MONITORING AGENCY NAME(S) AND ADDRESS(ES)
Office of Naval Research Global
86 Blenheim Crescent
Ruislip MX HA4 7HB
United Kingdom

10. SPONSOR/MONITOR'S ACRONYM(S)
ONRG

11. SPONSOR/MONITOR'S REPORT NUMBER(S)
N/A

12. DISTRIBUTION/AVAILABILITY STATEMENT
Approved for Public Release; Distribution is Unlimited

13. SUPPLEMENTARY NOTES
DUNS No. 731652728, CAGE: SCJD6, PR No. 1000010293

14. ABSTRACT
In this research, we propose and investigate a novel concept of measuring sea ice thickness and dielectric properties in a non-destructive way from near-field EM measurements. We have developed several analytical methods and sea ice models to compute the EM fields analytically. The analytical results are verified with the help of a finite element simulation software. A neural network based deep learning method has been proposed to solve the inverse problem of retrieving the thickness and dielectric properties of ice from the given field data. Small scale practical experiments have also been performed with wood and ice. We believe, our work has fascinating prospects for large scale sea ice monitoring.

15. SUBJECT TERMS
Electromagnetic waves, low-frequecy, near-field, deep neural network, thickness estimation, sea ice modelling

16. SECURITY CLASSIFICATION OF:			17. LIMITATION OF ABSTRACT	18. NUMBER OF PAGES	19a. NAME OF RESPONSIBLE PERSON
a. REPORT	b. ABSTRACT	c. THIS PAGE			Dr. Mohammad Ariful Haque
					19b. TELEPHONE NUMBER *(Include area code)*
U	U	U	SAR	32	+8801687129593

INSTRUCTIONS FOR COMPLETING SF 298

1. REPORT DATE. Full publication date, including day, month, if available. Must cite at least the year and be Year 2000 compliant, e.g. 30-06-1998; xx-06-1998; xx-xx-1998.

2. REPORT TYPE. State the type of report, such as final, technical, interim, memorandum, master's thesis, progress, quarterly, research, special, group study, etc.

3. DATE COVERED. Indicate the time during which the work was performed and the report was written, e.g., Jun 1997 - Jun 1998; 1-10 Jun 1996; May - Nov 1998; Nov 1998.

4. TITLE. Enter title and subtitle with volume number and part number, if applicable. On classified documents, enter the title classification in parentheses.

5a. CONTRACT NUMBER. Enter all contract numbers as they appear in the report, e.g. F33315-86-C-5169.

5b. GRANT NUMBER. Enter all grant numbers as they appear in the report. e.g. AFOSR-82-1234.

5c. PROGRAM ELEMENT NUMBER. Enter all program element numbers as they appear in the report, e.g. 61101A.

5e. TASK NUMBER. Enter all task numbers as they appear in the report, e.g. 05; RF0330201; T4112.

5f. WORK UNIT NUMBER. Enter all work unit numbers as they appear in the report, e.g. 001; AFAPL30480105.

6. AUTHOR(S). Enter name(s) of person(s) responsible for writing the report, performing the research, or credited with the content of the report. The form of entry is the last name, first name, middle initial, and additional qualifiers separated by commas, e.g. Smith, Richard, J, Jr.

7. PERFORMING ORGANIZATION NAME(S) AND ADDRESS(ES). Self-explanatory.

8. PERFORMING ORGANIZATION REPORT NUMBER. Enter all unique alphanumeric report numbers assigned by the performing organization, e.g. BRL-1234; AFWL-TR-85-4017-Vol-21-PT-2.

9. SPONSORING/MONITORING AGENCY NAME(S) AND ADDRESS(ES). Enter the name and address of the organization(s) financially responsible for and monitoring the work.

10. SPONSOR/MONITOR'S ACRONYM(S). Enter, if available, e.g. BRL, ARDEC, NADC.

11. SPONSOR/MONITOR'S REPORT NUMBER(S). Enter report number as assigned by the sponsoring/ monitoring agency, if available, e.g. BRL-TR-829; -215.

12. DISTRIBUTION/AVAILABILITY STATEMENT. Use agency-mandated availability statements to indicate the public availability or distribution limitations of the report. If additional limitations/ restrictions or special markings are indicated, follow agency authorization procedures, e.g. RD/FRD, PROPIN, ITAR, etc. Include copyright information.

13. SUPPLEMENTARY NOTES. Enter information not included elsewhere such as: prepared in cooperation with; translation of; report supersedes; old edition number, etc.

14. ABSTRACT. A brief (approximately 200 words) factual summary of the most significant information.

15. SUBJECT TERMS. Key words or phrases identifying major concepts in the report.

16. SECURITY CLASSIFICATION. Enter security classification in accordance with security classification regulations, e.g. U, C, S, etc. If this form contains classified information, stamp classification level on the top and bottom of this page.

17. LIMITATION OF ABSTRACT. This block must be completed to assign a distribution limitation to the abstract. Enter UU (Unclassified Unlimited) or SAR (Same as Report). An entry in this block is necessary if the abstract is to be limited.